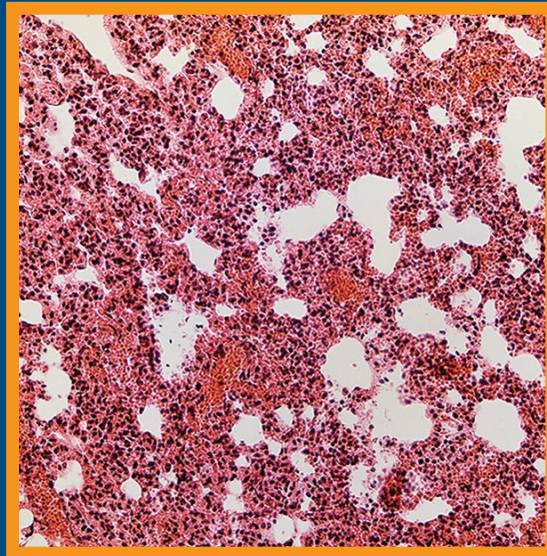


Folia Histochemica et Cytobiologica

Scientific quarterly devoted to problems of histochemistry,
cytochemistry and cell & tissue biology

www.fhc.viamedica.pl



Vol. 57

No. 4

2019

ISSN 0239-8508



VIA MEDICA

Folia Histochemica et Cytobiologica

Scientific quarterly devoted to problems of histochemistry,
cytochemistry and cell & tissue biology

www.fhc.viamedica.pl

EDITOR-IN CHIEF:

Z. Kmiec (Gdansk, Poland)

EDITORS:

M. Piasecka (Szczecin, Poland)

M.Z. Ratajczak (Louisville, USA)

J. Thekkiniath (New Haven, USA)

EDITORIAL BOARD:

C.E. Alpers (Seattle, USA)

B. Bilinska (Cracow, Poland)

I.-D. Caruntu (Iassi, Romania)

J.R. Couchman (Copenhagen, Denmark)

M. Dietel (Berlin, Germany)

P. Dziegiel (Wroclaw, Poland)

T. Fujimoto (Nagoya, Japan)

J. Kawiak (Warsaw, Poland)

J.Z. Kubiak (Rennes, France)

J.A. Litwin (Cracow, Poland)

C. Lucini (Naples, Italy)

A. Lukaszyk (Poznan, Poland)

Z. Mackiewicz (Vilnius, Lithuania)

A. Mazur (Clermont-Ferrand, France)

I. Petersen (Jena, Germany)

A.T. Slominski (Memphis, USA)

C.J.F. van Noordan (Amsterdam, Netherlands)

Y. Wegrowski (Reims, France)

S. Wolczynski (Bialystok, Poland)

M. Zabel (Poznan, Poland)

V. Zinchuk (Kochi, Japan)

M. J. Zeromski (Poznan, Poland)

M.A. Zmijewski (Gdansk, Poland)

MANAGING EDITOR:

C. Kobierzycki (Wroclaw, Poland)

PUBLISHER EDITOR:

I. Hallmann (Gdansk, Poland)

EDITORIAL OFFICE:

Department of Histology

Medical University of Gdansk

Debinki St. 1, 80–210 Gdansk, Poland

tel.: + 48 58 349 14 37

fax: + 48 58 349 14 19

e-mail: zkmiec@gumed.edu.pl

<http://www.fhc.viamedica.pl>

Folia Histochemica et Cytobiologica (pISSN 0239–8508, eISSN 1897–5631) is published quarterly, one volume a year, by the Polish Society for Histochemistry and Cytochemistry at VM Media sp. z.o.o VM Group sp.k., Gdansk.

Indexed in: Index Medicus/MEDLINE, Excerpta Medica/EMBASE, Chemical Abstracts/CAS, SCI Expanded, SciSearch, Biochemistry & Biophysics Citation Index, ISI Alerting Services, Biosis Previews Index Copernicus, Biological Abstracts, SCOPUS, Research Alert, ProQuest, EBSCO, DOAJ, Ulrich's Periodicals Directory.

POLISH SOCIETY FOR HISTOCHEMISTRY AND CYTOCHEMISTRY STATEMENT OF FOLIA HISTOCHEMICA ET CYTOBIOLOGICA EDITORIAL POLICY

Folia Histochemica et Cytobiologica is an international, English-language journal devoted to the rapidly developing fields of histochemistry, cytochemistry, cell and tissue biology.

The Folia Histochemica et Cytobiologica publishes papers that meet the needs and intellectual interests of medical professionals, basic scientists, college and university teachers and students. Prospective authors should read most recent issues of FHC to determine the appropriateness of a possible contribution. However, such an examination does not provide an infallible guide because editorial policy is always under review. Technical correctness is necessary, but it is not the only condition for acceptance. Clarity of exposition and potential interest of the readers are important considerations; it is the reader, not the author, who must receive the benefit of the doubt.

Folia Histochemica et Cytobiologica publishes review articles, original articles, short communications and proceedings of scientific congresses/symposia. Fields of particular interests include development and application of modern techniques in histochemistry and cell biology, cell biology and pathology, cell-microenvironment interactions, tissue organization and pathology.

Manuscripts announcing new theoretical or experimental results, or manuscripts questioning well-established and successful theories, are highly desirable and are a subject for evaluation by specialists. Manuscripts describing original research that clarifies past misunderstandings or allows a broader view of a subject are acceptable. Manuscripts that demonstrate new relations between apparently unrelated areas of fields of interests are appropriate. Manuscripts that show new ways of understanding, demonstrating, or deriving familiar results are also acceptable. Such manuscripts must provide some original cytobiological insight and not just a clever derivation.

Regularly, review or tutorial articles are published, often of a length greater than that of the average article. Most of these articles are a subject of a review; authors planning such articles are asked to consult with the editors at an early stage.

Most readers of a particular article will be specialists in the subject matter presented; the context within which the paper is presented should be established in the order given in Instructions for Authors. Manuscripts must be technically correct and must take proper cognizance of previous work on the same subject regardless of where it may have appeared. Such referencing is especially important for reminders of once well known ideas, proofs, or techniques that may have again become useful to readers. It is the responsibility of the author to provide adequate references; editors and referees will not do the literature search that should have been done by the authors. The references are a matter of review though.

Contributions considered include: Regular Articles (Papers), Short Communications, Review Articles, Conference Proceeding, Book Reviews and Technical Notes, which describe new laboratory methods or substantial improvements of the existing techniques. Regular articles should be about five journal pages or less in length. Short communications are usually confined to the discussion of a single concept and should be about two journal pages in length. Review articles are confined to a broad discussion and should contain the most recent knowledge about the subject.

Instructions concerning the preparation of manuscripts are given in the Information for Authors. Care in following those instructions will permit editors and referees to devote more time to thoughtful evaluation of contributions and will ultimately lead to a better, more interesting Journal.

Copying information, in part or in whole by any means is prohibited without a written permission from the owner.

SUBSCRIPTION

Folia Histochemica et Cytobiologica is available for paper subscription (print on demand).

To read and download articles for free as pdf document, visit <http://czasopisma.viamedica.pl/fhc>

Publisher: VM Media sp. z o.o. VM Group sp.k., Swietokrzyska St. 73, 80–180 Gdansk, <http://www.viamedica.pl>, wap.viamedica.pl

Illustration on the cover: *Acute lung injury in the mouse model of CLP-induced sepsis* (see: Li Meng *et al.*, pp. 168–178)

Legal note: <http://czasopisma.viamedica.pl/fhc/about/legalNote>

© Polish Society for Histochemistry and Cytochemistry



Folia Histochemica et Cytobiologica

Scientific quarterly devoted to problems of histochemistry,
cytochemistry and cell & tissue biology

www.fhc.viamedica.pl

Vol. 57

No. 4

2019

Official Journal of the Polish Society for Histochemistry and Cytochemistry

OBITUARY

Professor Stanisława Stokłosowa (1927–2019)

Barbara Bilinska, Jerzy Galas, Andrzej Lukaszuk, Jerzy Kawiak 155

COMMENTARY

Transforming growth factor- β activation in cell-free extracellular matrix preparations. Commentary

John R. Couchman..... 157

ORIGINAL PAPERS

In vitro evaluation of electroporated gold nanoparticles and extremely-low frequency electromagnetic field anticancer activity against Hep-2 laryngeal cancer cells

Mohammed A. Alshehri, Piotr M. Wierzbicki, Hassan F. Kaboo, Mohamed S.M. Nasr, Mohamed E. Amer, Tamer M.M. Abuamara, Doaa A. Badr, Kamel A. Saleh, Ahmed E. Fazary, Aly F. Mohamed..... 159

MiR-539-5p alleviates sepsis-induced acute lung injury by targeting ROCK1

Li Meng, Haohao Cao, Chunhua Wan, Lintao Jiang 168

Increased expression of CART, nNOS, VIP, PACAP, SP and GAL in enteric neurons of the porcine stomach prepyloric region following hydrochloric acid infusion

Jaroslav Calka..... 179

Professor Stanisława Stokłosowa (1927–2019)

The Polish Society for Histochemistry and Cytochemistry has been deeply affected by the announcement that Professor Stanisława Stokłosowa passed away on October 20, 2019. She was a meritorious member of the Society which conferred the distinction of Honorary Member on her in 1995. Her efforts to organize the Polish Branch of the European Tissue Culture Society, which actively acted as the Tissue Culture Section of the Polish Society for Histochemistry and Cytochemistry cannot be overlooked.



Professor Stanisława Stokłosowa was born on February 8, 1927 in Dobczyce near Krakow, Lesser Poland. During World War II, she attended undergraduate classes at the secondary school of humanities in Myślenice. Then she studied biology at the Faculty of Mathematics and Natural Sciences of the Jagiellonian University in Krakow where she graduated with a MSc thesis (1949) completed in the Department of Zoology. From 1949 till 1997 Professor Stokłosowa continuously worked in the Department of Animal Physiology in the Institute of Zoology, Jagiellonian University.

In 1962 she completed her PhD dissertation, and in 1972 obtained her “habilitation”, a higher degree qualifying for an associate professor. In 1974, she was appointed Reader and in 1980 — Professor.

We highly value the opportunity to present her accomplishments and pay tribute to them. She founded the Laboratory of Endocrinology and Tissue Culture and headed this unit until her retirement (1962–1997). Today her Laboratory exists as the Department of Endocrinology, Institute of Zoology and Biomedical Research, Faculty of Biology, Jagiellonian University in Krakow.

In co-operation with Charles University and the Czechoslovak Academy of Sciences in Prague, she published two pioneering papers in which she demonstrated sexual dimorphism in the structure of skin of

the bull trout. They have become classics in the body of scientific literature.

Professor Stanisława Stokłosowa had a long-term research stay at the University of Illinois, Urbana-Champaign, USA, where she was trained in radiocompetitive and radioimmunological assays of steroid hormones. She later adapted them for use in Krakow. At that time, Professor Stokłosowa gathered around her a group of young scientists and students and initiated studies on the isolation and culture of theca cells of the

ovary which offered a new *in vitro* research model. The results are often cited as pioneering studies. Developing the theca cell culture model enabled studies of interactions among different types of ovarian cells in co-cultures and of the regulation of hormonal function in isolated follicular ovarian cells. In 1976, she extended her studies to the model of isolated Leydig cells and Sertoli testicular cells. In 1980, studies of the effects of prolactin on various components of the ovary were initiated. These data were the first, providing an important contribution regarding the role of prolactin in reproduction. At the same time she commenced a pioneering study on the hormonal function of ovarian follicles isolated from seasonally reproducing rodents.

This line of *in vitro* research supplemented by histochemical, immunocytochemical, immunohistochemical and radioimmunological methods were important for building a good reputation for the Tissue Culture Laboratory in Poland and abroad. In these years her Laboratory was among the first Polish research units introducing these methods. Hence, there was a continuous influx of researchers and technicians from various domestic and foreign institutions, coming for training in these methods, which for years were valuable methodological foundations of the research in Professor Stokłosowa’s lab.

In the 1980s in a joint project with the Department of Molecular Genetics at the Czechoslovak Academy of Sciences in Prague, research was initiated on the localization of cytoskeletal elements in gonadal cells. To achieve this, immunocytochemical methods with monoclonal antibodies against tubulin α and β and vimentin were used. In cooperation with the Department of Ichthyobiology and Fisheries at the Academy of Agriculture in Krakow, Professor Stokłosowa adapted fish ovarian cells to tissue culture and performed studies on the hormonal regulation of steroidogenesis in the annual cycle. Moreover, she initiated a project on dynamics and hormonal regulation of androgen, estradiol and progesterone receptors in ovarian tissues.

Professor Stokłosowa cooperated with the Institute of Animal Reproduction and Food Research of the Polish Academy of Sciences (PAN) in Olsztyn, the Institute of Animal Physiology and Nutrition of PAN in Jabłonna, the Department of Molecular Genetics, Prague, the Research Institute of Animal Production, Uhřetíněves near Prague, the Department of Steroid Biochemistry in Glasgow, Scotland, the Institute of Hormone and Fertility Research, Hamburg, Germany, and the University of Caen, Laboratory of Biochemistry, Caen, France. She organized symposia with international participation on cell and tissue culture in the frame of her section within the Polish Society for Cytochemistry and Histochemistry. During the Symposium *Progress in techniques of cell and molecular biology* organized in Poznan (2000) her plenary lecture on the tissue culture models confirmed conference attendees how an invaluable role plays the cell culture system in histochemical studies.

The scientific output of Professor Stokłosowa comprises more than one hundred publications on the physiology and endocrinology of ovaries. She is the author of the textbook "Cell and Tissue Culture" published in Polish by the Polish Scientific Publisher (PWN) which has played a role of an indispensable

guide to the newcomers to these techniques. She kindly shared her wide knowledge and experience when teaching younger coworkers and students. She supervised 52 Master of Science theses, eight graduate students preparing their Ph.D. dissertations and five post-docs applying for habilitation (*veniam legendi*).

The scientific accomplishments of Professor Stanisława Stokłosowa and her position as a founder of the Cracow school of endocrinology of reproduction were awarded with the Jagiellonian Laurel by the Rector of the Jagiellonian University. The Polish state authorities honored her with Medal of the National Education Commission. In recognition of her scientific achievements and long-lasting cooperation between the scientific units in Olsztyn and her home University in Krakow she was awarded the doctor *honoris causa* title by the Senate of the Warmia and Mazury University in Olsztyn, Poland.

Finally, it is worth mentioning that Professor Stokłosowa's enormous efforts to found the international journal *Reproductive Biology* were successful. The official journal of the Society for Biology of Reproduction was launched in 2000 and she was the first Editor-in Chief until 2012.

Stanisława Stokłosowa was a stimulating and generous teacher, always open to suggestions and ever ready to provide a hypothesis and explanations with good will and humor. In addition to her passion for science, Professor Stokłosowa was an enthusiastic painter, loved flowers, still lifes, and portraits. In 2017, to celebrate her 90th birthday the exhibition of her paintings was organized in Collegium Maius of the Jagiellonian University in Krakow.

Her scientific, academic and editorial activities may be a significant message for early-stage researchers and future generations of scientists. Even after her death, Professor Stokłosowa's ideas and efforts are continuously promulgated and used by others.

Let her memory be eternal...

Barbara Bilinska, Jerzy Galas,
Andrzej Lukaszuk, and Jerzy Kawiak

Submitted: 20 December, 2019

Accepted after reviews: 20 December, 2019

Available as AoP: 20 December, 2019

Transforming growth factor- β activation in cell-free extracellular matrix preparations. Commentary

John R. Couchman

Biotech Research & Innovation Centre, University of Copenhagen, Denmark

Abstract

Transforming growth factor- β (TGF- β) is an important regulator of many cellular and immunological functions. It is often deposited in extracellular matrices in a latent form. This commentary is to draw attention to the likelihood that preparing cell-free matrices from tissue cultures by high pH buffers, such as ammonium hydroxide, can activate the TGF- β . Therefore, cells subsequently seeded onto such matrices may respond to the presence of active TGF- β in addition to interactions with macromolecular extracellular matrix components. (*Folia Histochemica et Cytobiologica* 2019, Vol. 57, No. 4, 157–158)

Key words: TGF- β ; latent TGF-binding protein; cell free ECM; high pH buffers

As far back as the 1980s the roles of extracellular matrix (ECM) components in regulating cell behaviour became increasingly popular. In addition to reductionist work in isolating and carefully characterising individual matrix macromolecules, efforts were made to assess whole matrices. Gospodarowicz's group identified several methods to grow cell monolayers to confluency, allowing them to assemble extracellular matrices, then removing the cells to leave the matrix for analysis, or to seed other cells on them [1–3]. Among these techniques, low concentrations of detergent, such as Triton X-100 together with hypotonic solutions containing ammonium hydroxide were developed. This high pH method is effective, and little cell debris remains attached to the matrices that are left largely intact.

At that time, little was known about transforming growth factor- β (TGF- β), but in the succeeding few years it became apparent that this important growth factor is expressed in a latent form. Activation of TGF- β could be achieved in various ways, and early experiments with soluble, medium-derived growth factor showed that extremes of pH were highly effective

[4–6]. Subsequently, a number of more physiologically relevant mechanisms to activate TGF- β have been characterised, including proteases, thrombospondin-1, reactive oxygen species and several integrin receptors [5, 7–10].

Further developments in the field showed that latent TGF- β could be inserted into the extracellular matrix through its interaction with large latent TGF-binding proteins (LTBPs), of which four distinct types are now known in mammals [11]. In this way the ECM serves as a reservoir of latent TGF- β by virtue of its association with a structural matrix component, *i.e.* LTBP [12, 13].

What appears to have escaped widespread attention is that preparation of cell-free matrices from cell cultures through the use of ammonium hydroxide can activate matrix-associated TGF- β . Therefore, cells subsequently seeded onto matrices prepared in this way will encounter not only matrix components, interacting with integrins, syndecans, CD44 *etc.*, but also activated TGF- β . Many years ago we found that matrices prepared from PF-HR9 mouse endodermal cells by alkali treatment would inhibit subsequently seeded mink lung epithelial cells (Mv1Lu) (M. Austria & J. Couchman, unpublished results). It is well known that TGF- β inhibits the proliferation of these cells [14], and in our case the inhibition could be overcome by TGF- β -specific blocking antibodies.

Even today current methods describe the use of 20 mM ammonium hydroxide (sometimes in PBS with

Correspondence address: John R. Couchman
Biotech Research & Innovation Centre,
University of Copenhagen, Denmark
Biocentre 1.3.16, Ole Maaløes Vej 5,
2200 Copenhagen N, Denmark
e-mail: john.couchman@bric.ku.dk

detergent [15, 16], or more usually in hypotonic conditions without detergent [17]), to prepare cell-free matrices, but there is no mention of the possibility that latent TGF- β can be activated by this method. I have often encountered young scientists who use this method and many are surprised when I advise them that it can result in the activation of the matrix-associated TGF- β . Therefore, the purpose of this commentary is to bring this aspect of matrix biology to scientists' attention. Where this is a key issue, other methods at neutral pH can be used, such as 2 M urea together with non-ionic detergents and hypotonic buffers [3, 17].

References

- Gospodarowicz D, Ili C. The extracellular matrix and the control of proliferation of corneal endothelial and lens epithelial cells. *Exp Eye Res.* 1980; 31(2): 181–199, doi: [10.1016/0014-4835\(80\)90077-9](https://doi.org/10.1016/0014-4835(80)90077-9), indexed in Pubmed: [7428843](https://pubmed.ncbi.nlm.nih.gov/7428843/).
- Gospodarowicz D, Hirabayashi K, Giguère L, et al. Factors controlling the proliferative rate, final cell density, and life span of bovine vascular smooth muscle cells in culture. *J Cell Biol.* 1981; 89(3): 568–578, doi: [10.1083/jcb.89.3.568](https://doi.org/10.1083/jcb.89.3.568), indexed in Pubmed: [6454694](https://pubmed.ncbi.nlm.nih.gov/6454694/).
- Gospodarowicz D, Gonzalez R, Fujii DK. Are factors originating from serum, plasma, or cultured cells involved in the growth-promoting effect of the extracellular matrix produced by cultured bovine corneal endothelial cells? *J Cell Physiol.* 1983; 114(2): 191–202, doi: [10.1002/jcp.1041140208](https://doi.org/10.1002/jcp.1041140208), indexed in Pubmed: [6218176](https://pubmed.ncbi.nlm.nih.gov/6218176/).
- Lawrence DA, Pircher R, Jullien P. Conversion of a high molecular weight latent beta-TGF from chicken embryo fibroblasts into a low molecular weight active beta-TGF under acidic conditions. *Biochem Biophys Res Commun.* 1985; 133(3): 1026–1034, doi: [10.1016/0006-291x\(85\)91239-2](https://doi.org/10.1016/0006-291x(85)91239-2), indexed in Pubmed: [3866579](https://pubmed.ncbi.nlm.nih.gov/3866579/).
- Lyons RM, Keski-Oja J, Moses HL. Proteolytic activation of latent transforming growth factor-beta from fibroblast-conditioned medium. *J Cell Biol.* 1988; 106(5): 1659–1665, doi: [10.1083/jcb.106.5.1659](https://doi.org/10.1083/jcb.106.5.1659), indexed in Pubmed: [2967299](https://pubmed.ncbi.nlm.nih.gov/2967299/).
- Munger JS, Harpel JG, Gleizes PE, et al. Latent transforming growth factor-beta: structural features and mechanisms of activation. *Kidney Int.* 1997; 51(5): 1376–1382, doi: [10.1038/ki.1997.188](https://doi.org/10.1038/ki.1997.188), indexed in Pubmed: [9150447](https://pubmed.ncbi.nlm.nih.gov/9150447/).
- Schultz-Cherry S, Murphy-Ullrich JE. Thrombospondin causes activation of latent transforming growth factor-beta secreted by endothelial cells by a novel mechanism. *J Cell Biol.* 1993; 122(4): 923–932, doi: [10.1083/jcb.122.4.923](https://doi.org/10.1083/jcb.122.4.923), indexed in Pubmed: [8349738](https://pubmed.ncbi.nlm.nih.gov/8349738/).
- Barcellos-Hoff MH, Dix TA. Redox-mediated activation of latent transforming growth factor-beta 1. *Mol Endocrinol.* 1996; 10(9): 1077–1083, doi: [10.1210/mend.10.9.8885242](https://doi.org/10.1210/mend.10.9.8885242), indexed in Pubmed: [8885242](https://pubmed.ncbi.nlm.nih.gov/8885242/).
- Wipff PJ, Hinz B. Integrins and the activation of latent transforming growth factor beta1 - an intimate relationship. *Eur J Cell Biol.* 2008; 87(8-9): 601–615, doi: [10.1016/j.ejcb.2008.01.012](https://doi.org/10.1016/j.ejcb.2008.01.012), indexed in Pubmed: [18342983](https://pubmed.ncbi.nlm.nih.gov/18342983/).
- Hinz B. It has to be the α : myofibroblast integrins activate latent TGF- β 1. *Nat Med.* 2013; 19(12): 1567–1568, doi: [10.1038/nm.3421](https://doi.org/10.1038/nm.3421), indexed in Pubmed: [24309651](https://pubmed.ncbi.nlm.nih.gov/24309651/).
- Rifkin DB, Rifkin WJ, Zilberberg L. LTBP in biology and medicine: LTBP diseases. *Matrix Biol.* 2018; 71-72: 90–99, doi: [10.1016/j.matbio.2017.11.014](https://doi.org/10.1016/j.matbio.2017.11.014), indexed in Pubmed: [29217273](https://pubmed.ncbi.nlm.nih.gov/29217273/).
- Taipale J, Miyazono K, Heldin CH, et al. Latent transforming growth factor-beta 1 associates to fibroblast extracellular matrix via latent TGF-beta binding protein. *J Cell Biol.* 1994; 124(1-2): 171–181, doi: [10.1083/jcb.124.1.171](https://doi.org/10.1083/jcb.124.1.171), indexed in Pubmed: [8294500](https://pubmed.ncbi.nlm.nih.gov/8294500/).
- Dallas SL, Miyazono K, Skerry TM, et al. Dual role for the latent transforming growth factor-beta binding protein in storage of latent TGF-beta in the extracellular matrix and as a structural matrix protein. *J Cell Biol.* 1995; 131(2): 539–549, doi: [10.1083/jcb.131.2.539](https://doi.org/10.1083/jcb.131.2.539), indexed in Pubmed: [7593177](https://pubmed.ncbi.nlm.nih.gov/7593177/).
- Cheifetz S, Weatherbee JA, Tsang ML, et al. The transforming growth factor-beta system, a complex pattern of cross-reactive ligands and receptors. *Cell.* 1987; 48(3): 409–415, doi: [10.1016/0092-8674\(87\)90192-9](https://doi.org/10.1016/0092-8674(87)90192-9), indexed in Pubmed: [2879635](https://pubmed.ncbi.nlm.nih.gov/2879635/).
- Vlodavsky I. Preparation of extracellular matrices produced by cultured corneal endothelial and PF-HR9 endodermal cells. *Curr Protoc Cell Biol.* 2001; Chapter 10: Unit 10.4, doi: [10.1002/0471143030.cb1004s01](https://doi.org/10.1002/0471143030.cb1004s01), indexed in Pubmed: [18228298](https://pubmed.ncbi.nlm.nih.gov/18228298/).
- Franco-Barraza J, Beacham DA, Amatangelo MD, et al. Preparation of extracellular matrices produced by cultured and primary fibroblasts. *Curr Protoc Cell Biol.* 2016; 71: 10.9.1–10.9.34, doi: [10.1002/cpcb.2](https://doi.org/10.1002/cpcb.2), indexed in Pubmed: [27245425](https://pubmed.ncbi.nlm.nih.gov/27245425/).
- Hellewell AL, Rosini S, Adams JC. A Rapid, Scalable method for the isolation, functional study, and analysis of cell-derived extracellular matrix. *J Vis Exp.* 2017(119), doi: [10.3791/55051](https://doi.org/10.3791/55051), indexed in Pubmed: [28117783](https://pubmed.ncbi.nlm.nih.gov/28117783/).

Submitted: 28 October, 2019

Accepted after reviews: 28 October, 2019

Available as AoP: 19 November, 2019

In vitro evaluation of electroporated gold nanoparticles and extremely-low frequency electromagnetic field anticancer activity against Hep-2 laryngeal cancer cells

Mohammed A. Alshehri¹, Piotr M. Wierzbicki², Hassan F. Kaboo³,
Mohamed S.M. Nasr³, Mohamed E. Amer⁴, Tamer M.M. Abuamara³,
Doaa A. Badr⁵, Kamel A. Saleh¹, Ahmed E. Fazary^{5*}, Aly F. Mohamed^{6**}

¹Department of Biology, Science Collage, King Khalid University, Abha, Saudi Arabia

²Department of Histology, Medical University of Gdansk, Gdansk, Poland

³Histology Department, Faculty of Medicine, Al-Azhar University, Cairo, Egypt

⁴Histology Department, Faculty of Medicine, Al-Azhar University, Damietta, Egypt

⁵Applied Research Department, Research & Development Sector, Egyptian Organization for Biological Products and Vaccines (VACSERA Holding Company), Giza, Egypt

⁶The International Center for Advanced Researches (ICTAR-Egypt), Cairo, Egypt

Abstract

Introduction. The extremely-low frequency electromagnetic field (ELFEMF) has been proposed for use in cancer therapy since it was found that magnetic waves interfere with many biological processes. Gold nanoparticles (Au-NPs) have been widely used for drug delivery during cancer in vitro studies due to their low cytotoxicity and high biocompatibility. The electroporation of cancer cells in a presence of Au-NPs (EP Au-NPs) can induce cell apoptosis, alterations of cell cycle profile and morphological changes. The impact of ELFEMF and EP Au-NPs on morphology, cell cycle and activation of apoptosis-associated genes on Hep-2 laryngeal cancer cell line has not been studied yet.

Materials and methods. ELFEMF on Hep-2 cells were carried out using four different conditions: 25/50 mT at 15/30 min, while Au-NPs were used as direct contact (DC) or with electroporation (EP, 10 pulses at 200V, equal time intervals of 4 sec). MTT assay was used to check the toxicity of DC Au-NPs. Expression of *CASP3*, *P53*, *BAX* and *BCL2* genes was quantified using qPCR. Cell cycle was analyzed by flow cytometry. Hematoxylin and eosin (HE) staining was used to observe cell morphology.

Results. Calculated IC_{50} of DC Au-NPs 24.36 μ M (4.79 μ g/ml) and such concentration was used for further DC and EP AuNPs experiments. The up-regulation of pro-apoptotic genes (*CASP3*, *P53*, *BAX*) and decreased expression of *BCL2*, respectively, was observed for all analyzed conditions with the highest differences for EP AuNPs and ELFEMF 50 mT/30 min in comparison to control cells. The highest content of cells arrested in G2/M phase was observed in ELFEMF-treated cells for 30 min both at 25 or 50 mT, while the cells treated with EP AuNPs or ELFEMF 50 mT/15 min showed highest ratios of apoptotic cells. HE staining of electroporated cells and cells exposed to ELFEMF's low and higher frequencies for different times showed nuclear pleomorphic

Correspondence address: *Professor Ahmed E, Fazary
Applied Research Department, Research & Development
Sector, Egyptian Organization for Biological Products and
Vaccines (VACSERA Holding Company),
51 Wezaret El-Zeraa St., Agouza, Giza, Egypt
e-mail: aefazary@gmail.com

<https://orcid.org/0000-0002-2614-4104>

**Professor Aly Fahmy Mohamed
The International Center for Advanced Researches
(ICTAR-Egypt), Cairo, Egypt
e-mail: fahmy.aly@gmail.com

cells. Numerous apoptotic bodies were observed in the irregular cell membrane of neoplastic and necrotic cells with mixed euchromatin and heterochromatin.

Conclusions. Our observations indicate that treatment of Hep-2 laryngeal cancer cells with ELFEMF for 30 min at 25–50 mT and EP Au-NPs can cause cell damage inducing apoptosis and cell cycle arrest. (*Folia Histochemica et Cytobiologica* 2019, Vol. 57, No. 4, 159–167)

Key words: gold nanoparticles; electroporation; extremely-low frequency electromagnetic field; Hep-2 cells; apoptosis; qPCR

Introduction

Laryngeal cancer most often refers to squamous cell carcinoma of the larynx. Other malignant tumors of the larynx (e.g., sarcoma, lymphoma, neuroendocrine tumors) are extremely rare in comparison. This disease consists of malignant tumors of mucosal origin that originate from the supra-glottis, glottis, and sub-glottis. Electromagnetic fields (EMFs) have been employed as useful tools in medical diagnosis. Recently, the use of EMFs has been expanded for therapeutic purposes because their interactions with living matter produce effects that initiate, accelerate or inhibit biological processes. Frequencies below 300 Hz are known as extremely low-frequency electromagnetic fields (ELFEMFs) which do not break molecular bonds due to low energy; therefore not causing direct DNA damage. Additionally, ELFEMFs are non-invasive and non-ionizing and even have non-thermal effects on cells and tissues. These properties have led to studies on the influence of ELFEMF on the development of various diseases, including cancer. While some researchers associate ELFEMF exposure with carcinogenesis [1, 2], other studies on experimental models and human cancers have shown that ELFEMF does not increase the risk of development of several tumor types, including liver cancer [3–5]. The ELFEMF treatment with tumor-specific frequencies is feasible and well-tolerated and may show positive biological efficacy in patients with advanced tumors [3–5]. Moreover, the exposure of female C3H/HeJ mice bearing human mammary adenocarcinoma to a frequency of 120 Hz at intensities of 4 and 5 mT resulted in a significant reduction in the growth of the tumors, which is a phenomenon associated with inhibition of angiogenesis [6]. Also, the exposure of female athymic nude mice with human breast cancer xenografts to a frequency of 120 Hz with an intensity of 15 mT, either alone or in combination with gamma radiation, resulted in decreased growth or reduced vascularization of the tumors [7]. Similarly, the effect of 50 Hz at 0.5 μ T and 0.5 mT on the development of chemically induced foci in rat livers showed a slight inhibition of foci formation [8]. Further studies on

ELFEMFs' impact on cancer cells are demanded since the current observations are insufficient as a proof of ELFEMF inhibition of carcinogenesis. The anticancer activity of gold nanoparticles (Au-NPs) has been studied against Dalton's lymphoma ascites (DLA) cell lines, human epithelial type 2 (Hep-2) cell lines and human leukemic monocyte lymphoma respectively [9, 10]. The anticancer effect of silver and gold nanoparticles against HepG-2 and lung cancer (A549) cell lines was performed [11, 12]. The results showed a good cytotoxic activity against the tested cancer cell lines. The concentration of Au-NPs plays an important role in their anticancer activity. Au-NPs showed expected effects against A549 cells in wide spectrum of concentrations: 100, 1 g, by 50 μ g, 25 μ g and 1 μ g. The lowest inhibitory effect on cells was observed for the concentration of 10 μ g. The cytotoxic effect of Au-NPs is the result of active physicochemical interaction of gold atoms with the functional groups of intracellular proteins, as well as with the nitrogen bases and phosphate groups in DNA. So, the aim of this study was to use electroporation in a presence of Au-NPs and ELFEMF effect on laryngeal carcinoma cell line (Hep-2) to evaluate genetic alteration under the effect of both electroporated Au-NPs and ELFEMF at different time and frequencies and related pathological changes [7].

Materials and methods

Cell culture. Laryngeal adenocarcinoma cell line (Hep-2, ATCC: CCL-23) was kindly supplied from the Holding company, Tissue Culture Department, for production of vaccines, sera, and drugs (VACSERA, Giza, Egypt). Cells were maintained in MEM-E medium supplemented with 10% fetal bovine serum (GIBCO, Thermo Fisher Scientific, Waltham, MA, USA) in a humidified atmosphere of 5% CO₂ at 37°C (Jouan SA, Saint-herblain, Pays de la Loire, France). Cells were maintained according to manufacturing protocol where the growth medium was decanted and cells were washed with phosphate buffer saline (Adwia Pharmaceuticals, El Sharkeya, Egypt). Cells were treated with 0.25% trypsin enzyme and 0.05% (v/v) EDTA (GIBCO) for 5 min at 37°C. Detached cells were splatted according to need.

Cell Viability and Au-NPs IC₅₀ evaluation (MTT Assay).

Cytotoxicity was conducted according to the previous work [13] where human laryngeal cancer cells were propagated in 75 cm² cell culture (TPP-Swiss) as previously mentioned according to the previously reported work [13]. Cells were plated at a concentration of 2×10^5 cell/ml in 96-well cell culture plates and incubated at 37°C for 24 h to achieve confluence. The growth medium was decanted and fresh medium containing 2 fold serially diluted Au-NPs dispensed to pre-cultured plate. 24 hrs later, dead cells were washed out using phosphate buffer saline (PBS, pH = 7.2 ± 0.2 (Adwia) and 50 μ l of MTT (3-(4,5-dimethylthiazol-2-yl)-2,5-diphenyltetrazolium bromide) stock solution (0.5 mg/ml) were added per well. After 4 h incubation period at 37°C, the supernatant was discarded and the formazan precipitate was solubilized by addition of 50 μ l/well of dimethyl sulfoxide (DMSO). Plates were incubated in the dark for 30 min at 37°C and absorbance was determined at a wavelength of 570 nm using microplate reader (ELx-800, Bio-Tek Instruments, Inc, Winooski, VT, USA). The cell viability percentage was calculated using the following formula: Viability percentage (%) = Mean OD of test dilution \times 100/ Mean OD of control wells. The IC₅₀ value was determined using GraphPad Prism software (v.6, GraphPad Software, La Jolla, CA, USA). For cell cycle and apoptotic profile, Hep-2 cells were pre-cultured in 25 cm² surface area (SA) cell culture flasks, treated with the IC₅₀ of Au-NPs in MEM-E medium post decanting the growth medium. 24 h later the affected cells were collected and divided for cell cycle and genetic analysis, the cells were harvested and fixed gently with 70% (v/v) ethanol in PBS, maintained at a temperature of 4°C overnight, and re-suspended in PBS containing 40 μ g/ml PI (propidium iodide), 0.1 mg/ml RNase and 0.1% (v/v) Triton X-100 in a dark room. After 30 min at 37°C, the cells were analyzed using a flow cytometer (Becton-Dickinson, San Jose, CA, USA) equipped with an argon ion laser at a wavelength of 488 nm. The cell cycle and sub-G1 group were determined and analyzed, as described previously.

Electroporation of laryngeal cancer cells. Hep-2 cells were seeded in 75 cm² cell culture flasks and incubated at 37°C (5% CO₂) until attachment. Cells were trypsinized and pelleted using cold centrifugation (Jouan-Ki21, ParisTech, France), the supernatant was decanted and Au-NPs (0.5 μ M/ mL) were added to 0.5 mL of Hep-2 cells and mixed well. Cells – Au-NPs (at the final concentration calculated as IC₅₀ for DC AuNPs) mix was placed in the sterile MicroPulsor electroporation cuvette (Biorad, Hercules, CA, USA). Ten pulses were made at 200V and applied to the cells at equal time intervals of 4 s. Negative control was considered.

Extremely-low frequency electromagnetic field treatment (ELFEMF). Four sterile test tubes of detached Hep-2 cancer

cell line (2×10^6 cell/ml/tube) were categorized, where two of the tubes were subjected to the electromagnetic field as 25 mT for 15 and 30 mins in a cooling atmosphere. The other two tubes were exposed to the electromagnetic field at 50 mT for the same time intervals. The apparatus (Medical Physics, Swiss Tropical and Public Health Institute, Basel, Switzerland) was adjusted for each magnetic field frequency using a teslameter set for justification of a magnetic field. The test tubes were kept inside the center of the coil producing EMF. The test tubes were tested for apoptotic profile regarding the pro-and anti-apoptotic genes (P53, Bcl-2, Bax, caspase-3), cell cycle and histological profile were considered.

Hematoxylin and eosin staining of Hep-2 cells. Fifty microliters of Au-NPs electroporated and ELFEMF exposed cells were dispensed on clean slides (3 for each treatment). Slides were air-dried, methanol fixed and rehydrated in descending concentrations of alcohol (100%, 90%, 75% and 50%). Slides were washed in distilled water for 5 min. The slides were immersed in filtered hematoxylin (HE) stain for 3 min and washed with distilled water twice. Slides were immersed in filtered eosin stain for 5 seconds and washed with distilled water. Dried slides were immersed in xylene, mounted with Canada balsam then coverslips were placed and left to dry. Ten microscopic fields of each slide were photomicrographed using the power of 400 \times . This was done using a digital camera (Canon, Tokyo, Japan), which was mounted on a light microscope. Images were transferred to the computer system for analysis. Field selection was based on the presence of the highest number of apoptotic cells. The photomicrographs were qualitatively evaluated for the presence of morphological criteria of apoptosis.

Expression of apoptosis-related genes. Total RNA was extracted from control, ELFEMF (25/50 mT for 15 and 30 min), 1 mM Au-NPs direct contact and electroporated exposed cells, respectively using RNeasy Mini Kit (Qiagen, Germantown, MD, USA) according to manufacturer's instructions. The concentration of extracted RNA was evaluated using a Beckman dual spectrophotometer (Beckman Instruments, Ramsey, MN, USA). The expression level of apoptosis-related genes; *P53* (F: 5'-TCAGATCCTAGC GTCGAGCCC-3' & R: 5'-GGGTGTGGAATCAACCCACAG-3'), *BAX* (F: 5'-ATGGACGGGTCCGGGGAGCA-3' & R: 5'-CCCAGTTGAAGTTGCCGTCA-3') and *BCL2* (F: 5'-GTGAACTGGGGGAGGATTGT-3' & R: 5'-GGAGAAATCAAACAGAGGCC-3') *CASP3* (F: 5'-CTCGGTCTGGTACAGATGTCTGA-3' & R: (5'-CATGGCTCAGAAGCACACAAAC-3) and housekeeping gene; *ACTB* (F: 5'-AGCGAGCATCCCCAAAGTT-3' & R: 5'-GGGCACGAAGGCTCATCATT-3) were determined using real-time PCR. 10 ng of the extracted total RNA from each sample was used for cDNA synthesis using high capacity cDNA reverse transcriptase kit (Applied

Biosystems-Thermo Fischer Scientific, USA). The obtained cDNA was subsequently amplified using Sybr Green I PCR master kit (Thermo Fisher Scientific Inc., Lithuania) using Step One apparatus (Applied Biosystems), as follows: 10 min at 95°C for enzyme activation followed by 40 cycles of 15 s at 95°C, 20 s at 55°C and 30 s at 72°C for the amplification step. Changes in the expression of each target gene were normalized relative to the mean critical threshold (CT) values of β -actin as housekeeping gene by the Δ CT method.

Cell cycle analysis. Cell cycle distribution was examined by measuring the DNA content of nuclei labeled with propidium iodide (PI). Au-NPs electroporated and ELFEMF treated Hep-2 cells were pelleted by cold centrifugation (Jouan Ki-21-France), washed with 1 ml of cold PBS, centrifuged, and fixed in 70% cold ethanol at +4°C for 24 hrs. Subsequently, cells were washed twice and treated with RNase A (20 mg/ml) and PI (20 mg/ml), FITC conjugated Annexin-V according to the protocol described by the manufacturer for 30 min at 37°C in the dark. Finally, cell cycle distribution analysis was performed using flow cytometry and the percentages of cells at G1, S and G2/M phases were calculated by flow cytometry (Becton-Dickinson).

Statistical analysis. All experiments were carried out three independent times. Results were statistically analyzed using GraphPad Prism v. 6.07 (GraphPad Software, San Diego, CA, USA) with the following tests: t-test between 2 subgroups, one-way analysis of variance (ANOVA) between more than two subgroups, regression analysis and Spearman's correlation test. All results were presented as mean \pm SD. The difference was considered statistically significant at $P < 0.05$.

Results

The toxicity test of Au-NPs was performed on Hep-2 cells and the results were shown in Figure 1. Based on that, the calculated IC_{50} concentration was $24.36 \mu\text{M}$ /ml ($4.79 \mu\text{g}/\text{ml}$). Such concentration of Au-NPs was used in further experiments with electroporation (EP Au-NPs) or by direct contact between Au-NPs and Hep-2 cells (DC Au-NPs). The influence of ELFEMF on Hep-2 cells was carried out using four different magnetic induction/time values: 25 mT/15 min, 25 mT/30 min, 50 mT/15 min and 50 mT/30 min. The expression profile of three pro-apoptotic genes (*CASP3*, *P53*, *BAX*) and one anti-apoptotic gene (*BCL2*) of Au-NPs and ELFEMF treated cells showed statistically different ratios (Fig. 2). We found the highest expression of *CASP3*, *P53* and *BAX* genes in EP Au-NPs and ELFEMFs cells at 50 mT/30 min (Fig. 2 A, B, C). Moreover, the tendency of increas-

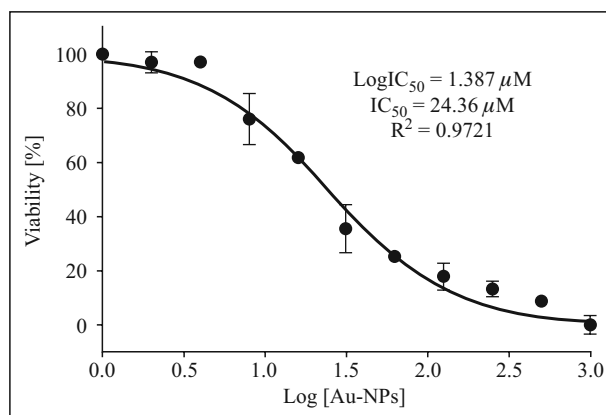


Figure 1. Evaluation of cytotoxicity of gold nanoparticles on Hep-2 cells using MTT assay. The calculated IC_{50} was $24.26 \mu\text{M}$ using Graphpad Prism software. The values obtained from three separate experiments are shown (mean \pm SD) and the nonlinear regression curve was added to plot, $R^2 = 0.972$.

ing expression of pro-apoptotic genes was observed in higher magnetic field/time values ($P > 0.05$, data not shown). We found that the electroporation with Au-NPs influenced the expression of *CASP3*, *P53* and *BAX* the similar way vs. direct contact with Au-NPs as increasing ELFEMF values. Regarding the *BCL2* gene, we did not observe the association between ELFEMF values and *BCL2* expression rate (except for the 25/15 vs. 50/30 mT/min values). Again, we found that EP Au-NPs-treated Hep-2 cells presented the lowest ratio of *BCL2* expression. The presented results showed that the electroporation with Au-NPs (at the concentration of $24.36 \mu\text{M}$) as well as the usage of ELFEMF at 50 mT/30 min values activated the expression of analyzed pro-apoptotic genes and deactivated the expression of anti-apoptotic *BCL2* gene at the highest values of tested conditions.

Next, we checked the influence of Au-NPs and ELFEMF on the cell cycle of Hep-2 cells (Fig. 3). The significant G2/M phase arrest was observed for cells treated with all ELFEMFs (except for 50 mT/15 min) values (Fig. 3C). It seems that the G2/M arrest was associated with prolonged time of exposure rather than higher dose of electromagnetic field. The similar pattern of ELFEMF impact was found in apoptotic cell distribution (Fig. 3D). Although the distribution of apoptotic cells in EP Au-NPs treated cells was higher than in control cells (Fig. 3D), we did not observed cellular arrest in any of analyzed cell cycle phases when cells were treated with gold nanoparticles.

The microscopic observation of ELFEMF exposed and Au-NPs electroporated cells showed morphologi-

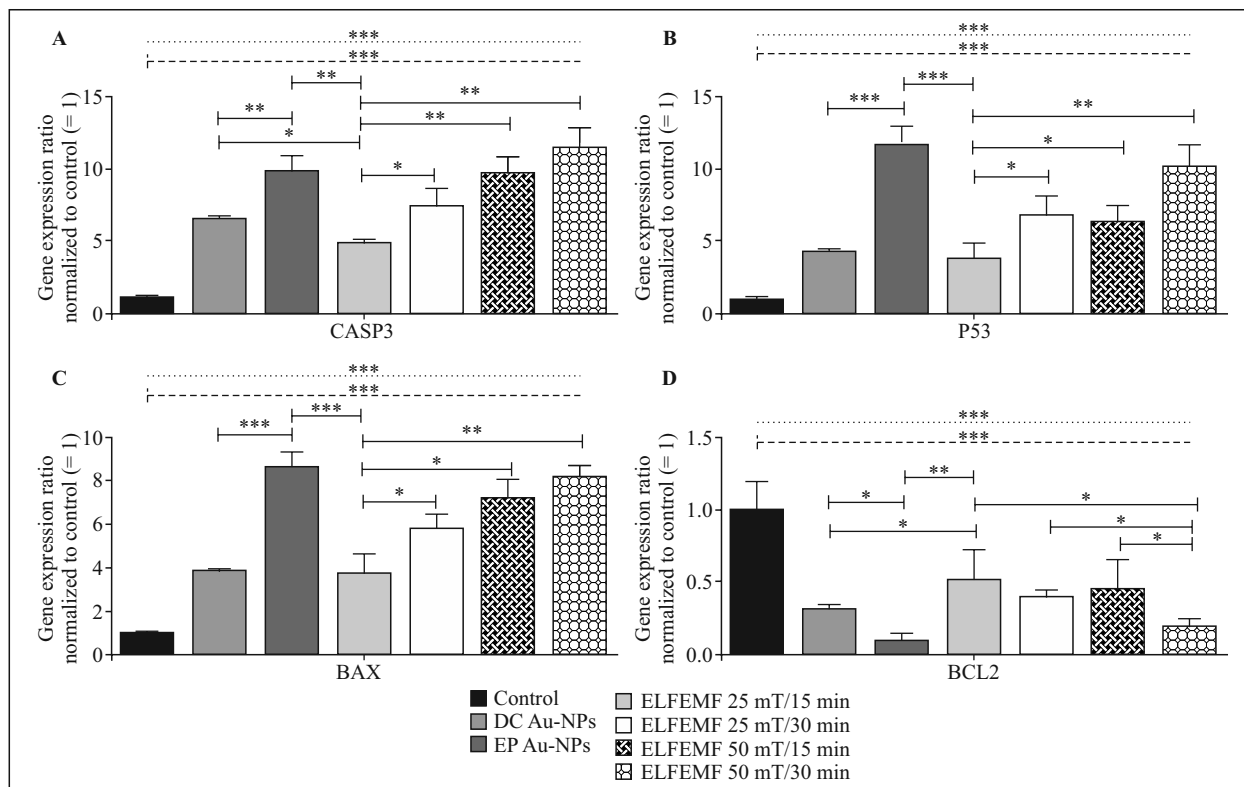


Figure 2. Expression analysis of the *CASP3*, *P53*, *BAX* and *BCL2* genes in Hep-2 cells at the mRNA level. Gene expression was assessed as described in the Materials and methods. (A–D) plots for *CASP3*, *P53*, *BAX* and *BCL2* genes' expression ratios in cells after treatment with different conditions, respectively. Bars and whiskers represent mean \pm standard deviation normalized to control samples. * $P < 0.05$, ** $P < 0.01$, *** $P < 0.001$; capped lines: t-test between subgroups; dotted line: one-way ANOVA between all subgroups; dashed line: t-test between control and tested cells, respectively. *CASP3*, caspase 3 gene; *P53*, tumor protein 53 gene; *BAX*, BCL2 associated X; *BCL2*, B-cell lymphoma 2 gene; DC Au-NPs, direct contact gold nanoparticles; EP Au-NPs, electroporation with gold nanoparticles; ELFEMF, extremely-low frequency electromagnetic field.

cal differences in comparison to control cells (Fig. 4). Hematoxylin and eosin staining of control, Hep-2 cells, showed regular cellular pleomorphic and nuclear pleomorphic cells (Fig. 4A), Au-NPs electroporated Hep-2 cells showed numerous apoptotic bodies, irregular cell membrane of neoplastic and necrotic cells with mixed euchromatin and heterochromatin (Fig. 4B). Also, Hep-2 cells showed numerous apoptotic bodies on post short term exposure to ELFEMF for 15 min at 25 mT and neoplastic cells with nuclear fragmentation and apoptotic body on post longer-term cell exposure (Fig. 4C); 30 min at 25 mT (Fig. 4D). Moreover, higher frequency at 50 mT for 15 min (Fig. 4E), exposed cells showed numerous apoptotic bodies and irregular neoplastic cell membrane and clear necrosis with mixed euchromatin and heterochromatin ruptured cell membrane of necrotic cells on post cell exposure to 50 mT for 30 min (Fig. 4F).

Discussion

The present work aimed to use ELFEMF and electroporation with Au-NPs as alternative ways of promotion apoptosis of human laryngeal cancer cells. Also, we aimed to preview the genetic and cell cycle alterations in Hep-2 cells. The obtained data revealed that both electroporation in a presence of Au-NPs and cell exposure to ELFEMF could manage the death of cancer cells *via* apoptosis induction.

The present study indicated that intermittent exposure of laryngeal carcinoma cells (Hep-2) to a 25 and 50 mT of ELFEMF affected cell cycle profile and proved these *via* noticed elevated up and down-regulation of apoptosis-related genes. Thus, we showed that apoptotic profile and G2/M cellular arrest may play the crucial role in the biological effects of 25 and 50 mT ELFEMF and related induction of DNA

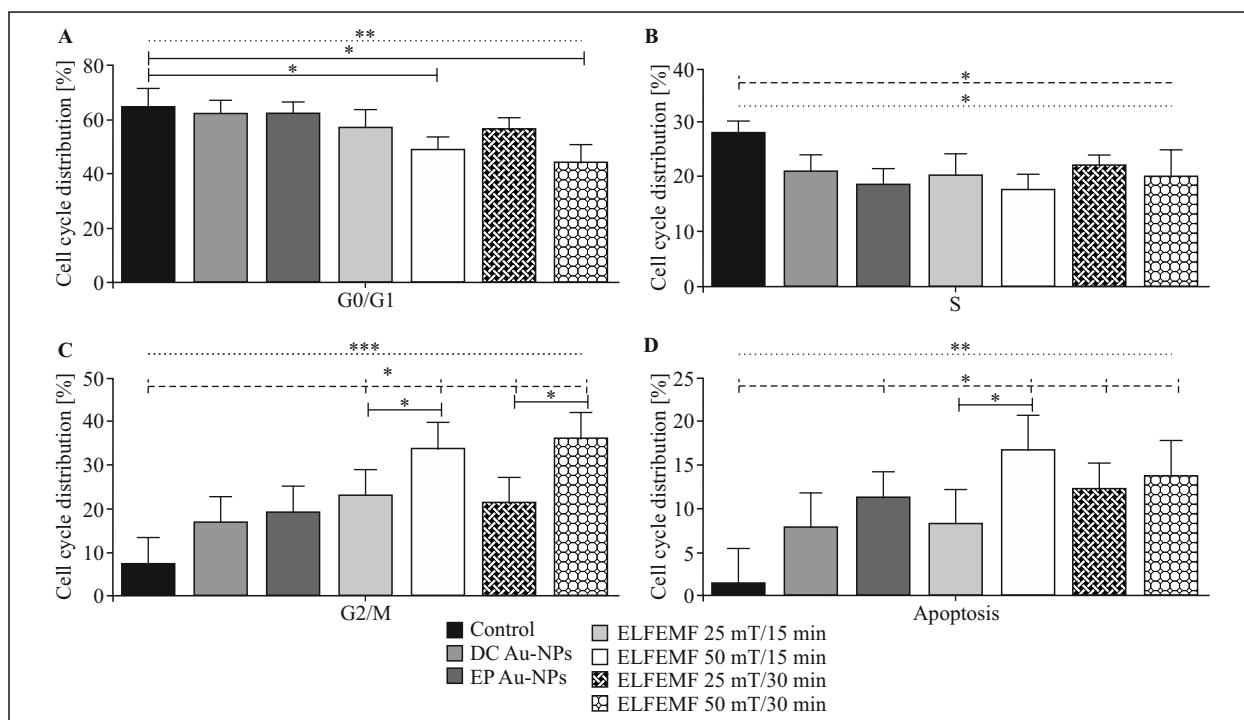


Figure 3. Evaluation of cell cycle of Hep-2 cells using flow cytometry. (A–D) G0/G1, S, G2/M phases and apoptotic cells' proportions of Hep-2 cells. * $P < 0.05$, ** $P < 0.01$, *** $P < 0.001$; capped lines: t-test between subgroups; dotted line: one-way ANOVA between all subgroups; dashed line: t-test between control and tested cells, respectively. DC Au-NPs, direct contact gold nanoparticles; EP Au-NPs, electroporation with gold nanoparticles; ELFEMF, extremely-low frequency electromagnetic field.

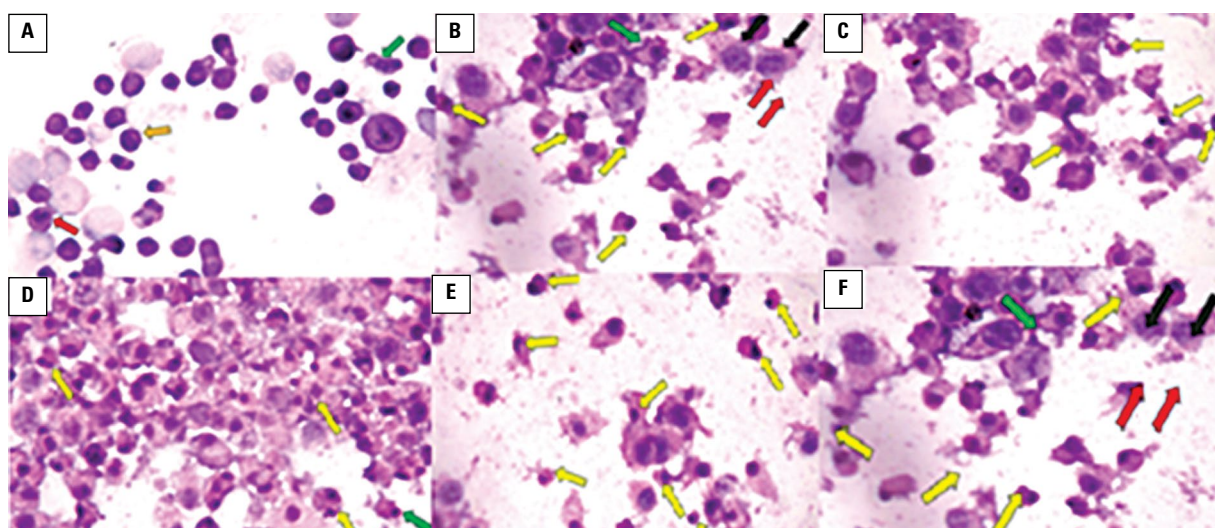


Figure 4. Microphotographs of Hep-2 cells after Au-NPs or ELFEMF treatment. A. Control, untreated Hep-2 cells present regular tumor cells (yellow arrow), cellular pleomorphism (green arrow) and nuclear pleomorphism (red arrow). B. Hep-2 Au-NPs electroporated cells show numerous apoptotic bodies (yellow arrows), irregular cell membrane of neoplastic cell (green arrow), necrotic cells with euchromatin and heterochromatin (red arrows) and ruptured cell membrane of necrotic cells (black arrows). C. Hep-2 cells showing numerous apoptotic bodies post short term exposure to ELFEMF for 15 min at 25 mT (yellow arrows). D. Hep-2 cells showing neoplastic cells with nuclear fragmentation (yellow arrows) and apoptotic bodies (green arrow) post cell exposure for 30 min at 25 mT. E. Hep-2 cells showing numerous apoptotic bodies (yellow arrows) after cell exposure to 50 mT for 15 min. F. Hep-2 cells showing numerous apoptotic bodies and irregular cell membrane of neoplastic cells (green arrow), necrotic cells (red arrows) and ruptured cell membrane of necrotic cells (black arrows) after cell exposure to 50 mT for 30 min. H&E staining, magnification $\times 40$.

strand breaks. On the other hand, it was observed that subjecting cells continuously to a constant electromagnetic field may induce adaptive mechanisms, protecting the genome from harmful influences [14]. The point of view concerning this way and effect was based on the continuous exposure of people to such frequencies *via* different magnetic field sources such as radio and microwave in their homes. The potential of ELFEMF to exert harmful biological effects on human health is of increasing concern. It has been reported that DNA damage may be involved in cell proliferation, apoptosis as well as cell cycle [15, 16].

The presence of Au-NPs inside the cells allowed the introduction and progress of cell damage, especially cancerous cells. On the other hand, it has been noticed that the cells that were exposed to the ELFEMF have developed a high rate of cellular damage. This cellular damage was developed by the irreversible induction of pores in the cell membrane due to the overlapping between the externally applied ELFEMF and the magnetic properties of the cell membranes. In addition to the effectiveness of the magnetic field on the cancerous cells, Au-NPs activate the signaling pathways through acting on the membrane proteins that leads to the inhibition of the cancer cells proliferation. It was previously observed that the gold nanoparticles have the ability to enter the cells through the endocytosis, which produces mitochondrial dysfunction, formation of reactive free radicals and the destruction of nucleic acid and cellular proteins [17]. Hence, all the used effects allow the inhibition of cellular proliferation. Therefore, the utilizing of gold nanoparticles in the presence of electroporation and the effect of extremely-low electromagnetic field has shown remarkable effects. This was done by the activation of Au-NPs to start entering the tumor cells, especially through electroporation physics enhancers accordingly displaying a remarkable ability to treat the tumor cells. It was observed that the use of electroporation in the presence of gold nanoparticles can be effective to induce apoptosis in the Hep-2 cells. Moreover, the combination of electroporation and Au-NPs had moderate effect on the studied neoplastic cells. Hence, the effect on pro-apoptotic genes (*P53* and *BAX*) and anti-apoptotic genes (*BCL2*) was viewed to be significant in the presence of combined action of gold nanoparticles and electroporation and the ELFEMF treatment with 50 mT and 100 mT.

The influence of size, shape, and surface modification on cytotoxicity of gold nanoparticles to human Hep-2 and canine MDCK cells was investigated by Zhang et al. [11]. Au-NPs cell treatment revealed that cell death induced predominately within one hour through apoptosis induced gene expression, whereas

cell death by free cetyltrimethylammonium-bromide (CTAB) was a time- and dose-dependent. Both positively and negatively surface-charged polymer-coated gold nanorods GNRs showed similar levels of cytotoxicity, suggesting the significance of surface functionality rather than surface charge in this case [11].

As the interaction of gold nanoparticles with cells relies on properties of nanoparticles, the cytotoxicity is complex and still under debate. In a previously published work, they found that cetyltrimethylammonium-bromide (CTAB) encapsulated gold nanorods (GNRs) were relatively higher cytotoxic than gold nanorods (GNRs) undergone further polymer coating and citrate stabilized gold nanospheres (GNSs) [11].

The toxicity of CTAB-encapsulated GNRs was mainly caused by CTAB on GNRs' surface but not free CTAB in the solution. On the contrary to our data, Brisdelli and coworkers recorded that lower frequency ELF-MF (1 mT; 50 Hz) enhanced the apoptosis and that ULEMF (25/50 mT; 50 Hz) enhanced the apoptosis and cell arrest in human laryngeal carcinoma Hep-2 cells [18]. Four different compounds, namely vinblastine, etoposide, quercetin, and resveratrol, enhanced apoptosis in human K562 chronic myeloid leukemia cells. The exposure to ELFEMF did not affect growth and viability of untreated K562 cells and did not influence the anti-proliferative effects of resveratrol, vinblastine, and etoposide [18]. On the contrary, in quercetin treated cells, exposure to ELFEMF significantly reduced the percentage of apoptotic cells and the caspase-3 activity and modified the cell cycle profile especially after 48 hours of exposure. In addition, the simultaneous treatments for 24 hours with quercetin plus ELFEMF increased Bcl-2 protein expression and prevented quercetin-induced downregulation of Mcl-1 and Bcl-xL [18].

The ELFEMF-dependent modulation of the expression of anti-apoptotic Bcl-2 family and Hsp70 proteins could act as a pro-survival mechanism in K562 cells [18]. ELFEMF seems to produce several biological effects such as changes in cell proliferation, cell differentiation, cell cycle and enzyme activity [19–22]. Moreover, ELFEMF was found to affect cellular redox homeostasis, modulation of physiological functions such as mitochondrial membrane potential, Ca^{+2} signaling and homeostasis, and ATP synthesis [23–25]. Alterations in the apoptosis process are involved in the pathogenesis of many types of cancer [26]. There is evidence implicating ELFEMF in the development of this disease in humans [27], and many *in vitro* studies have also reported correlation between apoptotic process and ELFEMF. The latter has been involved in the reduction or delay of cell apoptosis process, as well as in its stimulation [28, 29].

Additionally, some studies reported evidence suggesting the combined effects of ELFEMF and various chemicals and physical agents in modulating the apoptotic cascade [30, 31]. However, current research is characterized by conflicting data, and synergistic and/or antagonistic effect induced by ELFEMF has been described in H₂O₂-treated erythroleukemia cell line [32]. Also, our data was on the contrary of the previous work recording that the effects of 50 Hz ELFEMF exposure on the growth of GC-2 and cell viability was detected with the CCK-8 kit following 50 Hz ELFEMF exposure at different magnetic intensities for 72 hours to explore the effects of the ELFEMF on the growth of GC-2 cells [33]. Data showed that the 50 Hz ELFEMF did not markedly affect the morphology or viability (CCK-8) of GC-2 cells. Also, the effect of 50 Hz ELFEMF exposure on the apoptosis and cell cycle of GC-2 cells result showed that 50 Hz (ELFEMF) did not induce apoptosis in GC-2 cells compared with the same group [33]. Additionally, the percentages of G1-, S-, and G2-M phase cells did not significantly differ between the exposed groups post-treatment with 50 Hz ELFEMF for 72 hours. These findings confirmed that 50 Hz ELFEMF did not induce apoptosis or cell cycle arrest in GC-2 cell [34–36].

Based on the presented data, it could be concluded that the treatment of Hep-2 cancer cell with ELFEMF and electroporation with Au-NPs can cause cell damage inducing cell cycle arrest and apoptosis. Apoptotic and cell cycle profiles were cell type, time and ELFEMF frequency dependent. Usage of either Au-NPs-electroporation or ELFEMF in anti-cancer therapy may be a promising cancer therapy tool, may substitute or enhance the radio-, chemotherapy and surgical therapy approaches with least adverse effects. More intensified trials are recommended on different cancer cell lines as well as in vivo studies and different formulation of different nanoparticles shapes and concentrations must be validated.

Acknowledgement

The authors extend their appreciation to the Deanship of Scientific Research at King Khalid University, Abha, Saudi Arabia for funding this work through General Research Project under grant number G.R.P. 1/9/38-38.

References

- Girgert R, Schimming H, Körner W, et al. Induction of tamoxifen resistance in breast cancer cells by ELF electromagnetic fields. *Biochem Biophys Res Commun*. 2005; 336(4): 1144–1149, doi: [10.1016/j.bbrc.2005.08.243](https://doi.org/10.1016/j.bbrc.2005.08.243), indexed in Pubmed: [16168388](https://pubmed.ncbi.nlm.nih.gov/16168388/).
- Chen G, Upham BL, Sun W, et al. Effect of electromagnetic field exposure on chemically induced differentiation of friend erythroleukemia cells. *Environ Health Perspect*. 2000; 108(10): 967–972, doi: [10.1289/ehp.00108967](https://doi.org/10.1289/ehp.00108967), indexed in Pubmed: [11049817](https://pubmed.ncbi.nlm.nih.gov/11049817/).
- Barbault A, Costa FP, Bottger B, et al. Amplitude-modulated electromagnetic fields for the treatment of cancer: discovery of tumor-specific frequencies and assessment of a novel therapeutic approach. *J Exp Clin Cancer Res*. 2009; 28: 51, doi: [10.1186/1756-9966-28-51](https://doi.org/10.1186/1756-9966-28-51), indexed in Pubmed: [19366446](https://pubmed.ncbi.nlm.nih.gov/19366446/).
- Galloni P, Marino C. Effects of 50 Hz magnetic field exposure on tumor experimental models. *Bioelectromagnetics*. 2000; 21(8): 608–614, doi: [10.1002/1521-186x\(200012\)21:8<608::aid-bem7>3.0.co;2-z](https://doi.org/10.1002/1521-186x(200012)21:8<608::aid-bem7>3.0.co;2-z), indexed in Pubmed: [11102951](https://pubmed.ncbi.nlm.nih.gov/11102951/).
- Yasui M, Kikuchi T, Ogawa M, et al. Carcinogenicity test of 50 Hz sinusoidal magnetic fields in rats. *Bioelectromagnetics*. 1997; 18(8): 531–540, doi: [10.1002/\(sici\)1521-186x\(1997\)18:8<531::aid-bem1>3.0.co;2-3](https://doi.org/10.1002/(sici)1521-186x(1997)18:8<531::aid-bem1>3.0.co;2-3), indexed in Pubmed: [9383241](https://pubmed.ncbi.nlm.nih.gov/9383241/).
- Williams CD, Markov MS, Hardman WE, et al. Therapeutic electromagnetic field effects on angiogenesis and tumor growth. *Anticancer Res*. 2001; 21(6A): 3887–3891, indexed in Pubmed: [11911264](https://pubmed.ncbi.nlm.nih.gov/11911264/).
- Cameron IL, Sun LZ, Short N, et al. Therapeutic Electromagnetic Field (TEMF) and gamma irradiation on human breast cancer xenograft growth, angiogenesis and metastasis. *Cancer Cell Int*. 2005; 5: 23, doi: [10.1186/1475-2867-5-23](https://doi.org/10.1186/1475-2867-5-23), indexed in Pubmed: [16045802](https://pubmed.ncbi.nlm.nih.gov/16045802/).
- Rannug A, Holmberg B, Ekström T, et al. Rat liver foci study on coexposure with 50 Hz magnetic fields and known carcinogens. *Bioelectromagnetics*. 1993; 14(1): 17–27, doi: [10.1002/bem.2250140105](https://doi.org/10.1002/bem.2250140105), indexed in Pubmed: [8442779](https://pubmed.ncbi.nlm.nih.gov/8442779/).
- Sriram MI, Kanth SB, Kalishwaralal K, et al. Antitumor activity of silver nanoparticles in Dalton's lymphoma ascites tumor model. *Int J Nanomedicine*. 2010; 5: 753–762, doi: [10.2147/IJN.S11727](https://doi.org/10.2147/IJN.S11727), indexed in Pubmed: [21042421](https://pubmed.ncbi.nlm.nih.gov/21042421/).
- Repacholi MH, Greenebaum B. Interaction of static and extremely low frequency electric and magnetic fields with living systems: health effects and research needs. *Bioelectromagnetics*. 1999; 20(3): 133–160, doi: [10.1002/\(sici\)1521-186x\(1999\)20:3<133::aid-bem1>3.0.co;2-o](https://doi.org/10.1002/(sici)1521-186x(1999)20:3<133::aid-bem1>3.0.co;2-o), indexed in Pubmed: [10194557](https://pubmed.ncbi.nlm.nih.gov/10194557/).
- Zhang Y, Xu D, Li W, et al. Effect of size, shape, and surface modification on cytotoxicity of gold nanoparticles to human Hep-2 and canine MDCK cells. *J Nanomaterials*. 2012; 2012: 1–7, doi: [10.1155/2012/375496](https://doi.org/10.1155/2012/375496).
- Rajeshkumar S. Anticancer activity of eco-friendly gold nanoparticles against lung and liver cancer cells. *J Genet Eng Biotechnol*. 2016; 14(1): 195–202, doi: [10.1016/j.jgeb.2016.05.007](https://doi.org/10.1016/j.jgeb.2016.05.007), indexed in Pubmed: [30647615](https://pubmed.ncbi.nlm.nih.gov/30647615/).
- Lim HK, Asharani PV, Hande MP, et al. Cytotoxicity and genotoxicity of silver nanoparticles in human cells. *ACS Nano*. 2009; 3(2): 279–290, doi: [10.1021/nn800596w](https://doi.org/10.1021/nn800596w), indexed in Pubmed: [19236062](https://pubmed.ncbi.nlm.nih.gov/19236062/).
- Artacho-Cordón F, Salinas-Asensio Md, Calvente I, et al. Could radiotherapy effectiveness be enhanced by electromagnetic field treatment? *Int J Mol Sci*. 2013; 14(7): 14974–14995, doi: [10.3390/ijms140714974](https://doi.org/10.3390/ijms140714974), indexed in Pubmed: [23867611](https://pubmed.ncbi.nlm.nih.gov/23867611/).
- Kah JC, Wong KYi, Neoh KG, et al. Critical parameters in the pegylation of gold nanoshells for biomedical applications: an in vitro macrophage study. *J Drug Target*. 2009; 17(3): 181–193, doi: [10.1080/10611860802582442](https://doi.org/10.1080/10611860802582442), indexed in Pubmed: [19016072](https://pubmed.ncbi.nlm.nih.gov/19016072/).
- Bailon P, Won CY. PEG-modified biopharmaceuticals. *Expert Opin Drug Deliv*. 2009; 6(1): 1–16, doi: [10.1517/17425240802650568](https://doi.org/10.1517/17425240802650568), indexed in Pubmed: [19236204](https://pubmed.ncbi.nlm.nih.gov/19236204/).
- Behzadi S, Serpooshan V, Tao W, et al. Cellular uptake of nanoparticles: journey inside the cell. *Chem Soc Rev*. 2017; 46(14): 4218–4244, doi: [10.1039/c6cs00636a](https://doi.org/10.1039/c6cs00636a), indexed in Pubmed: [28585944](https://pubmed.ncbi.nlm.nih.gov/28585944/).

18. Brisdelli F, Bennato F, Bozzi A, et al. ELF-MF attenuates quercetin-induced apoptosis in K562 cells through modulating the expression of Bcl-2 family proteins. *Mol Cell Biochem.* 2014; 397(1-2): 33–43, doi: [10.1007/s11010-014-2169-1](https://doi.org/10.1007/s11010-014-2169-1), indexed in Pubmed: [25084985](https://pubmed.ncbi.nlm.nih.gov/25084985/).
19. Frederix F, Friedt JM, Choi KH, et al. Biosensing based on light absorption of nanoscaled gold and silver particles. *Anal Chem.* 2003; 75(24): 6894–6900, doi: [10.1021/ac0346609](https://doi.org/10.1021/ac0346609), indexed in Pubmed: [14670050](https://pubmed.ncbi.nlm.nih.gov/14670050/).
20. Hainfeld JF, Slatkin DN, Smilowitz HM. The use of gold nanoparticles to enhance radiotherapy in mice. *Phys Med Biol.* 2004; 49(18): N309–N315, doi: [10.1088/0031-9155/49/18/n03](https://doi.org/10.1088/0031-9155/49/18/n03), indexed in Pubmed: [15509078](https://pubmed.ncbi.nlm.nih.gov/15509078/).
21. Paciotti GF, Myer L, Weinreich D, et al. Colloidal gold: a novel nanoparticle vector for tumor directed drug delivery. *Drug Deliv.* 2004; 11(3): 169–183, doi: [10.1080/10717540490433895](https://doi.org/10.1080/10717540490433895), indexed in Pubmed: [15204636](https://pubmed.ncbi.nlm.nih.gov/15204636/).
22. Podsiadlo P, Sinani VA, Bahng JH, et al. Gold nanoparticles enhance the anti-leukemia action of a 6-mercaptopurine chemotherapeutic agent. *Langmuir.* 2008; 24(2): 568–574, doi: [10.1021/la702782k](https://doi.org/10.1021/la702782k), indexed in Pubmed: [18052300](https://pubmed.ncbi.nlm.nih.gov/18052300/).
23. Niidome T, Yamagata M, Okamoto Y, et al. PEG-modified gold nanorods with a stealth character for in vivo applications. *J Control Release.* 2006; 114(3): 343–347, doi: [10.1016/j.jconrel.2006.06.017](https://doi.org/10.1016/j.jconrel.2006.06.017), indexed in Pubmed: [16876898](https://pubmed.ncbi.nlm.nih.gov/16876898/).
24. Huang YC, Yang YC, Yang KC, et al. Pegylated gold nanoparticles induce apoptosis in human chronic myeloid leukemia cells. *Biomed Res Int.* 2014; 2014: 182353, doi: [10.1155/2014/182353](https://doi.org/10.1155/2014/182353), indexed in Pubmed: [24790990](https://pubmed.ncbi.nlm.nih.gov/24790990/).
25. Liu CJ, Wang CH, Chen ST, et al. Enhancement of cell radiation sensitivity by pegylated gold nanoparticles. *Phys Med Biol.* 2010; 55(4): 931–945, doi: [10.1088/0031-9155/55/4/002](https://doi.org/10.1088/0031-9155/55/4/002), indexed in Pubmed: [20090183](https://pubmed.ncbi.nlm.nih.gov/20090183/).
26. Chen HH, Chien CC, Petibois C, et al. Quantitative analysis of nanoparticle internalization in mammalian cells by high resolution X-ray microscopy. *J Nanobiotechnology.* 2011; 9: 14, doi: [10.1186/1477-3155-9-14](https://doi.org/10.1186/1477-3155-9-14), indexed in Pubmed: [21477355](https://pubmed.ncbi.nlm.nih.gov/21477355/).
27. Fruijtier-Pöllöth C. Safety assessment on polyethylene glycols (PEGs) and their derivatives as used in cosmetic products. *Toxicology.* 2005; 214(1-2): 1–38, doi: [10.1016/j.tox.2005.06.001](https://doi.org/10.1016/j.tox.2005.06.001), indexed in Pubmed: [16011869](https://pubmed.ncbi.nlm.nih.gov/16011869/).
28. Liu CJ, Yang TY, Wang CH, et al. Enhanced photocatalysis, colloidal stability and cytotoxicity of synchrotron X-ray synthesized Au/TiO₂ nanoparticles. *Materials Chemistry and Physics.* 2009; 117(1): 74–79, doi: [10.1016/j.matchemphys.2009.05.030](https://doi.org/10.1016/j.matchemphys.2009.05.030).
29. Liu CJ, Wang CH, Chien CC, et al. Enhanced x-ray irradiation-induced cancer cell damage by gold nanoparticles treated by a new synthesis method of polyethylene glycol modification. *Nanotechnology.* 2008; 19(29): 295104, doi: [10.1088/0957-4484/19/29/295104](https://doi.org/10.1088/0957-4484/19/29/295104), indexed in Pubmed: [21730596](https://pubmed.ncbi.nlm.nih.gov/21730596/).
30. Wang CH, Liu CJ, Wang CL, et al. Optimizing the size and surface properties of polyethylene glycol (PEG)–gold nanoparticles by intense x-ray irradiation. *J Physics D: Applied Physics.* 2008; 41(19): 195301, doi: [10.1088/0022-3727/41/19/195301](https://doi.org/10.1088/0022-3727/41/19/195301).
31. Wang CH, Liu CJ, Chien CC, et al. X-ray synthesized PEGylated (polyethylene glycol coated) gold nanoparticles in mice strongly accumulate in tumors. *Mat Chem Phys.* 2011; 126(1-2): 352–356, doi: [10.1016/j.matchemphys.2010.11.014](https://doi.org/10.1016/j.matchemphys.2010.11.014).
32. Nogueira-Pedro A, Cesário TA, Dias CC, et al. Hydrogen peroxide (H₂O₂) induces leukemic but not normal hematopoietic cell death in a dose-dependent manner. *Cancer Cell Int.* 2013; 13(1): 123, doi: [10.1186/1475-2867-13-123](https://doi.org/10.1186/1475-2867-13-123), indexed in Pubmed: [24365069](https://pubmed.ncbi.nlm.nih.gov/24365069/).
33. Liu Y, Liu Wb, Liu KJ, et al. Effect of 50 Hz extremely low-frequency electromagnetic fields on the DNA methylation and DNA methyltransferases in mouse spermatocyte-derived cell line GC-2. *Biomed Res Int.* 2015; 2015: 237183, doi: [10.1155/2015/237183](https://doi.org/10.1155/2015/237183), indexed in Pubmed: [26339596](https://pubmed.ncbi.nlm.nih.gov/26339596/).
34. Arellanes-Robledo J, Márquez-Rosado L, Pérez-Carreón JI, et al. Celecoxib induces regression of putative preneoplastic lesions in rat liver. *Anticancer Res.* 2006; 26(2A): 1271–1280, indexed in Pubmed: [16619534](https://pubmed.ncbi.nlm.nih.gov/16619534/).
35. Carrasco-Legleu CE, Márquez-Rosado L, Fattel-Fazenda S, et al. Chemoprotective effect of caffeic acid phenethyl ester on promotion in a medium-term rat hepatocarcinogenesis assay. *Int J Cancer.* 2004; 108(4): 488–492, doi: [10.1002/ijc.11595](https://doi.org/10.1002/ijc.11595), indexed in Pubmed: [14696111](https://pubmed.ncbi.nlm.nih.gov/14696111/).
36. Márquez-Rosado L, Trejo-Solís MC, García-Cuéllar CM, et al. Celecoxib, a cyclooxygenase-2 inhibitor, prevents induction of liver preneoplastic lesions in rats. *J Hepatol.* 2005; 43(4): 653–660, doi: [10.1016/j.jhep.2005.02.032](https://doi.org/10.1016/j.jhep.2005.02.032), indexed in Pubmed: [16023763](https://pubmed.ncbi.nlm.nih.gov/16023763/).

Submitted: 24 April, 2019

Accepted after reviews: 12 November, 2019

Available as AoP: 20 November, 2019

MiR-539-5p alleviates sepsis-induced acute lung injury by targeting ROCK1

Li Meng^{1*}, Haohao Cao^{2*}, Chunhua Wan¹, Lintao Jiang³

¹Departement of Anesthesiology, The Affiliated Hospital of Hubei Provincial Government, Wuhan, China

²Departement of Critical Care Medicine, Wuhan Forth Hospital, Wuhan, Hubei Province, 430000, China

³Departement of Emergency, Central Hospital of Wuhan, Wuhan, Hubei Province, 430000, China

*both authors equally contributed to this paper

Abstract

Introduction. Sepsis-induced acute lung injury (ALI) is an inflammatory process involved with simultaneous production of inflammatory cytokines and chemokines. In this study, we investigated the regulatory role of miR-539-5p in sepsis-induced ALI using a mouse model of cecal ligation puncture (CLP) and an *in vitro* model of primary murine pulmonary microvascular endothelial cells (MPVECs).

Material and methods. Adult male C57BL/6 mice were intravenously injected with or without miR-539-5p agomir or scrambled control one week before CLP operation. MPVECs were transfected with miR-539-5p mimics or control mimics, followed by lipopolysaccharide (LPS) stimulation. ROCK1 was predicted and confirmed as a direct target of miR-539-5p using dual-luciferase reporter assay. In rescue experiment, MPVECs were co-transfected with lentiviral vector expressing ROCK1 (or empty vector) and miR-539-5p mimics 24 h before LPS treatment. The transcriptional activity of caspase-3, the apoptosis ratio, the levels of miR-539-5p, interleukin-1 β (IL-1 β), interleukin-6 (IL-6), and ROCK1 were assessed.

Results. Compared to sham group, mice following CLP showed pulmonary morphological abnormalities, elevated production of IL-1 β and IL-6, and increased caspase-3 activity and apoptosis ratio in the lung. In MPVECs, LPS stimulation resulted in a significant induction of inflammatory cytokine levels and apoptosis compared to untreated cells. The overexpression of miR-539-5p in septic mice alleviated sepsis-induced pulmonary injury, apoptosis, and inflammation. MiR-539-5p also demonstrated anti-apoptotic and anti-inflammatory effect in LPS-treated MPVECs. The upregulation of ROCK1 in MPVECs recovered miR-539-5p-suppressed caspase-3 activity and proinflammatory cytokine production.

Conclusion. In conclusion, miR-539-5p alleviated sepsis-induced ALI *via* suppressing its downstream target ROCK1, suggesting a therapeutic potential of miR-539-5p for the management of sepsis-induced ALI. (*Folia Histochemica et Cytobiologica* 2019, Vol. 57, No. 4, 168–178)

Key words: mouse; acute lung injury; sepsis; inflammation; MPVEC cells; miRNA; ROCK1; caspase-3; cytokines

Correspondence address: Chunhua Wan
Department of Anesthesiology, The Central Hospital of Wuhan,
Unit 2, Building 23, Phase II, Yuejiazui Staff Residential
Quarter, No. 46, Joy Avenue,
Hongyuan District, Wuhan, Hubei, China
phone: 86+0278-2211435
e-mail: ChunhuaWanrui@163.com

Introduction

Sepsis is life-threatening syndrome characterized by an excessive systemic inflammatory response to infections induced by pathogenic bacteria, fungi, or viruses [1]. Patients with severe sepsis commonly present with microvascular thrombosis and subsequent multiple organ dysfunction [2]. Acute lung injury (ALI)

is a clinical syndrome consisting of a wide range of acute hypoxemic respiratory failure disorders and has become one of the most common complications of severe sepsis [3]. Pathophysiological studies revealed that the injury to the alveolar epithelium and pulmonary endothelial cells leads to an induction of epithelial permeability, pulmonary edema, and acute respiratory failure during the development of ALI [4]. However, no current available pharmacologic therapy has been recommended as a standard management of ALI [5].

Sepsis-induced ALI is an acute inflammatory process involved with simultaneous production of inflammatory cytokines and chemokines. Interleukin-1 β (IL-1 β), for example, has been found in bronchoalveolar lavage fluids from ALI patients [6]. In patients with persistent acute respiratory distress syndrome, a more severe form of ALI, the high ratio of IL-1 β to its antagonist suggested an essential role of IL-1 β in maintaining chronic inflammatory condition in lungs [7]. The other key step in ALI progression is the extensive apoptosis of alveolar epithelial cells, which has been considered as a primary cause of lung epithelium death in ALI patients [8]. Studies in murine endotoxin-induced lung injury models showed that the accumulation of soluble Fas ligand in Fas-dependent pathway induced apoptosis in lung epithelial cells [9, 10]. Thus, the blockage of inflammatory response and apoptotic signaling in the lung might be a useful therapeutic strategy in ameliorating sepsis-induced ALI.

MicroRNAs (miRNAs) are a class of small non-coding RNAs that have shown an emerging regulatory role in many pathological processes, including sepsis-induced organ dysfunction [11]. The overexpression of miR-146a attenuated sepsis-triggered myocardial dysfunction *in vitro* via inhibiting NF- κ B activation and the expression of inflammatory cytokines [12]. MiR-27a mediated the protective effect of paclitaxel in the damaged liver from septic mice by suppressing NF- κ B/TAB3 signaling pathway [13]. MiR-539-5p has been shown as a potent regulator in choroidal neovascularization and the migration of mesenchymal stem cells in fracture healing [14, 15]. However, whether it may exert beneficial effect in ALI remains unclear.

In this study, we aimed to investigate the regulatory role and potential molecular mechanism of miR-539-5p in sepsis-induced ALI by using a murine sepsis model and the primary murine pulmonary microvascular endothelial cells. The degree of lung tissue injury, the level of apoptosis and the expression of inflammatory cytokines were examined. Our findings may suggest a novel therapeutic approach in the management of septic ALI.

Materials and methods

Mouse model of sepsis. A total of 24 adult male C57BL/6 mice (28–32 g) were purchased from Charles River Laboratories China and maintained in a controlled environment (12 h alternating light-dark cycle, 22–24°C, 60% humidity) with *ad libitum* access to food and water. All experiments in this study were approved by the Animal Care and Use Committee of The Central Hospital of Wuhan, and performed following the Guide for the Care and Use of Laboratory Animals [16]. After one-week acclimatization, 18 mice underwent cecal ligation and puncture (CLP) surgery to establish the model of CLP-induced sepsis as previously described [17, 18]. In brief, mice were anesthetized by *i.p.* injection of 10% chloral hydrate (3 mL/kg, Sigma-Aldrich, St. Louis, MI, USA) and fixed on the operating table in supine position. A 4-mm longitudinal midline incision was made to expose the cecum. The exposed cecum was ligated at 10 mm from the tip using 3-0 silk sutures and then punctured once with a 20-gauge needle at 5 mm distal from the ligation. After extruding a small amount of feces by gently squeezing the cecum, the bowel was repositioned and the abdominal musculature, peritoneum and skin were closed using sterile sutures. Immediately after the surgery, 5 mL/100 g saline was subcutaneously injected for fluid resuscitation. Sham-operated mice (n = 6) underwent the same surgical procedure without the ligation or puncture of the cecum.

***In vivo* delivery of plasmid DNA.** CLP mice were randomly divided into three groups: CLP, CLP + NC agomir, and CLP + miR-539-5p agomir. The miRNA reagents, miR-539-5p agomir and scrambled control (NC agomir), were purchased from GenePharm (Shanghai, China) and mixed with linear polyethyleneimine (PEI) nanoparticles (Sigma-Aldrich) as previously described [19]. A total of 200 μ L mixture containing 5 nmol miRNA (miR-539-5p agomir or NC agomir) was intravenously injected *via* the tail vein into designated group one week before the CLP operation. Animals were euthanized with carbon dioxide asphyxia 24 h post-surgery. Lungs were harvested and stored properly for further analyses.

Histological analysis. The same portion of the lung samples in mice were used for histopathological examination. Tissues were fixed in 4% paraformaldehyde, embedded in paraffin, cut into 5 μ m sections, and then stained with hematoxylin and eosin (H&E). The degree of lung damage was estimated using lung injury scoring by an investigator blinded to the experiment as previously described [20]. Five randomly selected fields were scored *per* slide at magnification 400 \times .

Cell culture and transfection. Primary murine pulmonary microvascular endothelial cells (MPVECs) were isolated

and cultured in DMEM (Sigma-Aldrich) as previously described [21]. The miR-539-5p mimics and control mimics (50 nM) were synthesized by GenePharm and transfected into MPVECs using Lipofectamine 2000 (Invitrogen, Carlsbad, CA, USA). Twenty-four hours after transfection, cells were stimulated with 1 mg/mL lipopolysaccharide (LPS, Sigma-Aldrich). The transcriptional activity of caspase-3 was examined 30 min thereafter. The levels of miR-539-5p, interleukin-1 β (IL-1 β), interleukin-6 (IL-6), and ROCK1 were assessed 6 h following the LPS treatment. In rescue experiment, MPVECs were co-transfected with 1 μ g recombinant lentiviral vector expressing ROCK1 (or empty lentiviral vector) and 50 nM miR-539-5p mimics 24 h prior to the treatment with LPS. MPVECs co-transfected with empty lentiviral vector and control mimics were used as a control group.

Dual-luciferase reporter assay. ROCK1 3'-UTR fragment containing the putative binding site of miR-539-5p was amplified and cloned into the downstream of luciferase gene in the pmirGlo vector (GenePharm). The mutant ROCK1 3'-UTR was used to construct ROCK1-MUT vector. HEK-293 cells were plated into 12-well plates (Thermo Fisher Scientific, Waltham, MA, USA) and co-transfected with miR-539-5p mimics (or NC mimics) and ROCK1-WT (or ROCK1-MUT) at 70–80% confluency. The luciferase activities were assessed 2 days after the transfection using Dual-Luciferase Reporter Assay System (Promega Biotech Co., Madison, WI, USA).

Quantitative real-time PCR (qRT-PCR). Target miRNA was extracted from mice lung tissues and MPVECs using mirVana™ miRNA Isolation Kit (Invitrogen). The reverse transcription of miR-539-5p was performed using All-in-One™ miRNA RT-qPCR Detection Kit (GeneCopoeia Inc., Rockville, MD, USA). Total RNAs were isolated using Trizol LS (Invitrogen) and reverse transcribed to cDNA using the ReverTra Ace qPCR RT Kit (Toyobo, Osaka, Japan) according to the manufacturer's instructions. Target genes were amplified using 7300 Real-Time PCR System (Applied Biosystem, Foster City, CA, USA). The expression of miR-539-5p was normalized by U6, while β -actin was used as internal control for mRNA expression. The primers used in this study were: miR-539-5p: GGAGAAUUAUC-CUUGGUGUGU; U6 forward: CTCGCTTCGGCAG-CACA, U6 reverse: AACGCTTCACGAATTTGCGT; IL-1 β forward: CCAGGATGAGGACCCAAGCA, IL-1 β reverse: TCCCGACCATTGCTGTTTCC; IL-6 forward: TAGCCGCCCCACACAGACAG, IL-6 reverse: GGCT-GGCATTTGTGGTTGGG; ROCK1 forward: AAA-GAAAGGATGGAG-GATGAAGT, ROCK1 reverse: TGTAACAACAGCCGCTTATTTG; β -actin forward: AT-CACTGCCACCCAGAAGAC, β -actin reverse: TTTCTA-GACGGCAGGTCAGG.

Enzyme-linked immunosorbent assay (ELISA). Total proteins extracted from mice lung tissues and MPVEC lysates were prepared. Concentrations of IL-1 β and IL-6 were measured using ELISA kits (R&D Systems, Minneapolis, MN, USA) according to the manufacturer's protocol.

Transcriptional activity assay. The transcriptional activity of caspase-3 in mice lung tissues and MPVECs were evaluated using Caspase-3 Assay Kit (Abcam, Cambridge, UK) according to the manufacturer's protocol. Lung samples were homogenized in RIPA buffer with protease inhibitor (Bio-Rad Laboratories, Hercules, CA, USA). MPVECs were lysed in cell lysis buffer 30 min after LPS stimulation. The protein concentration in all samples were adjusted to 100–150 μ g protein per 50 μ L cell lysis buffer. The mixture of 50 μ L 2 \times Reaction Buffer and 10 mM DTT were added to 50 μ L sample, followed by the incubation with 5 μ L 4 mM DEVD-p-NA substrate at 37°C for 2 h. The optical density values for the peroxidase reaction product were measured at 450 nm using a microplate reader.

Apoptosis assay. Cell apoptosis was assessed using Annexin V-FITC Apoptosis Detection Kit (#14085, Abcam,) according to the manufacturer's instructions. Briefly, MPVECs were cultured in 6-well plates to reach 70–80% confluency followed by the transfection and LPS stimulation as mentioned above. After 24 h, cells were collected, centrifuged, and resuspended in 500 μ L 1 \times buffer solution at the concentration of 5×10^5 cells/mL. Then 5 μ L Annexin V-FITC and 5 μ L propidium iodide (PI) were added to the cells and incubated at room temperature for 5 min in the dark. The apoptosis ratio was quantified in the flow cytometry analysis using BD FACS software (BD Biosciences, San Jose, CA, USA).

Western blot. Total proteins (40–80 μ g) from MPVEC lysates were separated on an 8% SDS-PAGE gel under reducing conditions and then transferred to polyvinylidene fluoride membranes (MilliporeSigma, Burlington, MA, USA). After blocking, membranes were incubated with ROCK1 antibody (1:2000, #ab45171, Abcam) and β -catenin antibody (1:2000, #ab32572, Abcam) at 4°C for 6 h. After three washes with TBST buffer, membranes were incubated with goat anti-rabbit secondary antibody (1:3000, #ab6721, Abcam) for 45 min. Protein bands were visualized using Alphamager™ 2000 Imaging System (Alpha Innotech, San Leandro, CA, USA) and the density of bands was quantified.

Statistical analysis. Data in this study are presented as mean \pm standard deviation. The statistical significance was analyzed using two-tailed Student's t-test or one-way ANOVA (SPSS software, version 24.0, Chicago, IL, USA). A value of $p < 0.05$ was considered statistically significant.

All experiments were performed in triplicate and repeated three times.

Results

MiR-539-5p was downregulated in mice with CLP-induced sepsis and the overexpression of miR-539-5p alleviated CLP-induced lung injury

To study the regulatory role of miR-539-5p in sepsis-induced ALI, we established a mouse model of sepsis induced by CLP surgery. The induction of miR-539-5p expression in septic mice was achieved by intravenous injection of miR-539-5p agomir prior to CLP treatment. Compared to sham-operated group, the expression of miR-539-5p in the lung tissues was significantly inhibited following CLP surgery. The injection of miR-539-5p-expressing plasmid in septic mice significantly promoted the level of miR-539-5p compared to the ones administered with control miRNA (Fig. 1A). The degree of lung tissue damage was evaluated using lung injury scoring, in which miR-539-5p overexpression significantly improved the histological damage caused by CLP operation (Fig. 1B). As shown in the lung sections stained with H&E, sham-operated group showed morphologically normal structure of pulmonary alveoli. CLP mice, on the contrary, showed thickened alveolar walls and septa, collapsed alveolar sacs, visible vascular congestion and hemorrhage. The histopathological features in septic mice injected with control agomir were similar to those in CLP group. The induction of miR-539-5p alleviated the pulmonary alveoli damage induced by sepsis (Fig. 1C). These results suggested that miR-539-5p protected mice from sepsis-induced lung injury following CLP surgery.

Induction of miR-539-5p decreased apoptosis marker activity and proinflammatory cytokine production in the lung tissues of CLP mice

We found that the transcriptional activity of caspase-3 was significantly elevated in CLP-operated animals, whereas miR-539-5p overexpression induced a significant reduction of caspase-3 activity in septic mice (Fig. 2A). The expressions of IL-1 β and IL-6, two major proinflammatory cytokines, were significantly increased in septic animals at both mRNA and protein levels compared to sham-operated group. The induction of miR-539-5p in mice with ALI significantly suppressed the expressions of both cytokines (Fig. 2B–C). These results indicated that miR-539-5p ameliorated sepsis-induced apoptosis and proinflammatory cytokine production.

Overexpression of miR-539-5p reduced LPS-induced apoptosis and inflammation in MPVECs

In this study, we stimulated MPVECs with LPS to mimic pulmonary damage *in vitro*. LPS-treated cells demonstrated significantly lower level of miR-539-5p compared to untreated cells. Under the condition of LPS stimulation, wild-type MPVECs and the ones transfected with control mimics showed similar miR-539-5p level, whereas the delivery of miR-539-5p mimics significantly increased the expression of miR-539-5p (Fig. 3A). The caspase-3 activity was remarkably promoted by LPS treatment, while miR-539-5p overexpression resulted in a significant reduction of caspase-3 activity in LPS-treated MPVECs (Fig. 3B). LPS-induced secretion of IL-1 β and IL-6 in MPVECs was also significantly impeded by miR-539-5p (Fig. 3C–D). Flow cytometry data showed that LPS stimulated apoptosis in MPVECs, whereas the transfection of miR-539-5p mimics efficiently decreased the apoptosis ratio as compared to control mimics-transfected cells (Fig. 3E). The above findings suggested the anti-apoptotic and anti-inflammatory role of miR-539-5p *in vitro*.

ROCK1 was directly targeted by miR-539-5p

To explore the potential mechanisms underlying the involvement of miR-539-5p in ALI, we searched for the downstream target of miR-539-5p using bioinformatics analysis on TargetScan. ROCK1 was predicted as a direct target gene of miR-539-5p with a putative binding site (Fig. 4A). Dual-luciferase reporter assay showed that the luciferase activity of ROCK1-WT was significantly lower in cells transfected with miR-539-5p mimics compared to control mimics cells. In contrast, cells transfected with ROCK1-MUT reporter showed no difference on the luciferase activity between miR-539-5p mimics and control mimics groups (Fig. 4B). Then, we measured the mRNA and protein levels of ROCK1 in wild-type and miR-539-5p-overexpressing MPVECs and found that the expression of ROCK1 was significantly downregulated by the induction of miR-539-5p (Fig. 4C).

MiR-539-5p inhibited apoptosis and inflammatory responses via the suppression of ROCK1

To further investigate whether miR-539-5p regulated apoptosis and inflammation *via* targeting ROCK1, we co-transfected MPVECs with miR-539-5p mimics and lentiviral vector expressing ROCK1 (or empty vector). The transfection efficacy was confirmed by significantly augmented expressions of ROCK1 at both mRNA and protein levels in MPVECs transfected with

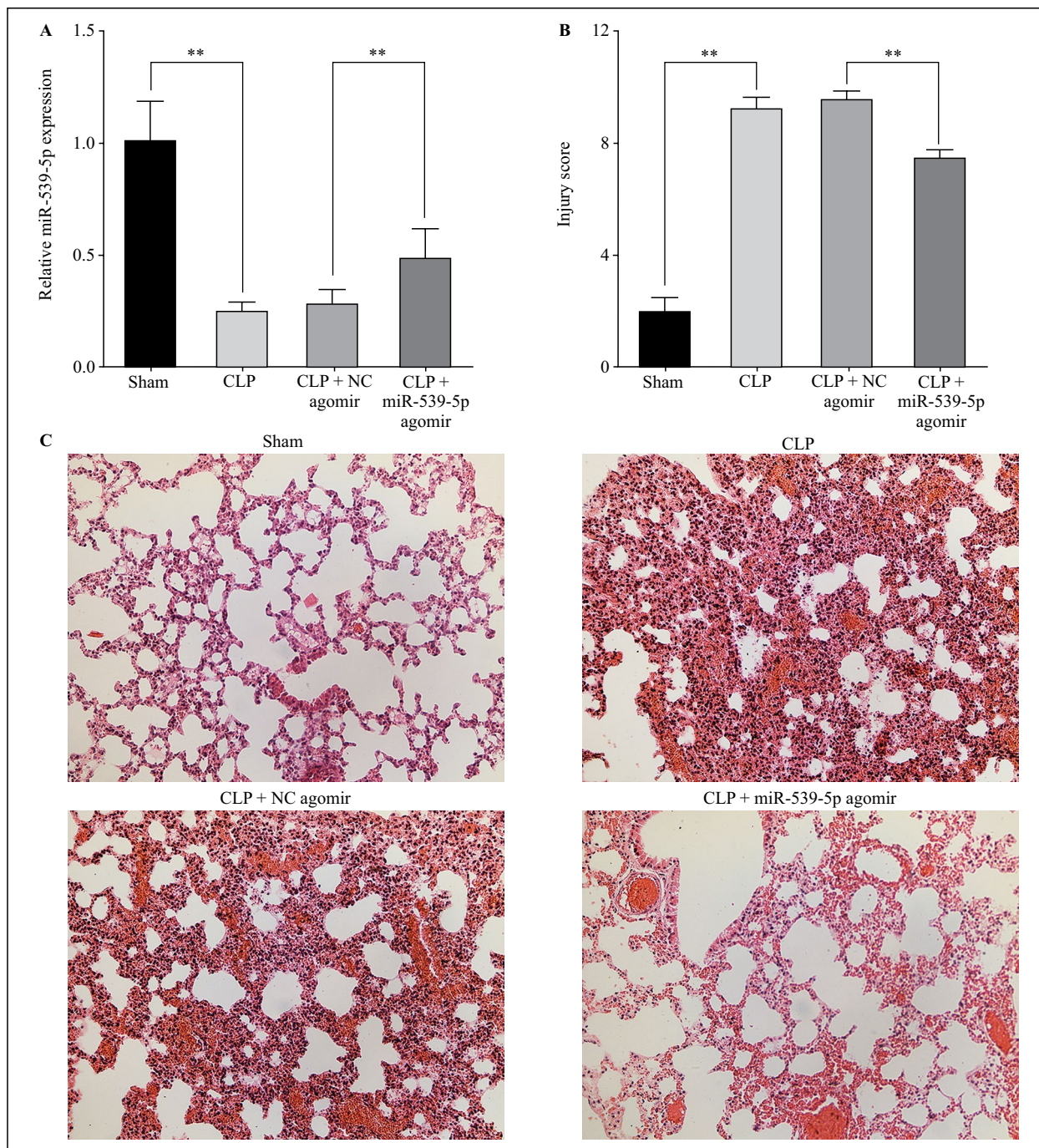


Figure 1. Pulmonary expression of miR-539-5p in the mouse model of CLP-induced sepsis and the effect of miR-539-5p overexpression on sepsis-induced lung injury. Adult male C57BL/6 mice were divided into four groups: CLP, CLP + NC agomir, CLP + miR-539-5p, and sham group ($n = 6$ in each group). Animals in CLP, CLP + NC agomir, CLP + miR-539-5p groups were intravenously injected with vehicle, scrambled miRNA control, and miR-539-5p agomir, respectively, followed by CLP surgery. Sham group underwent the same surgical procedure of CLP without the ligation or puncture of the cecum. All animals were euthanized 24 h after the surgery, and their lung tissues were collected. **A.** Pulmonary expression of miR-539-5p was examined using qRT-PCR. **B.** Sectioned lung tissue samples were stained with H&E and the degree of lung damage was determined using lung injury scoring. **C.** Representative histological images were shown ($400\times$ magnification). $**p < 0.01$.

ROCK1 vector (Fig. 5A–B). We further explored the effect of ROCK1 overexpression on apoptosis and inflammation in MPVECs carrying miR-539-5p mimics.

Compared to control cells, MPVECs co-transfected with miR-539-5p and empty vector showed significantly impaired caspase-3 activity. The induction of

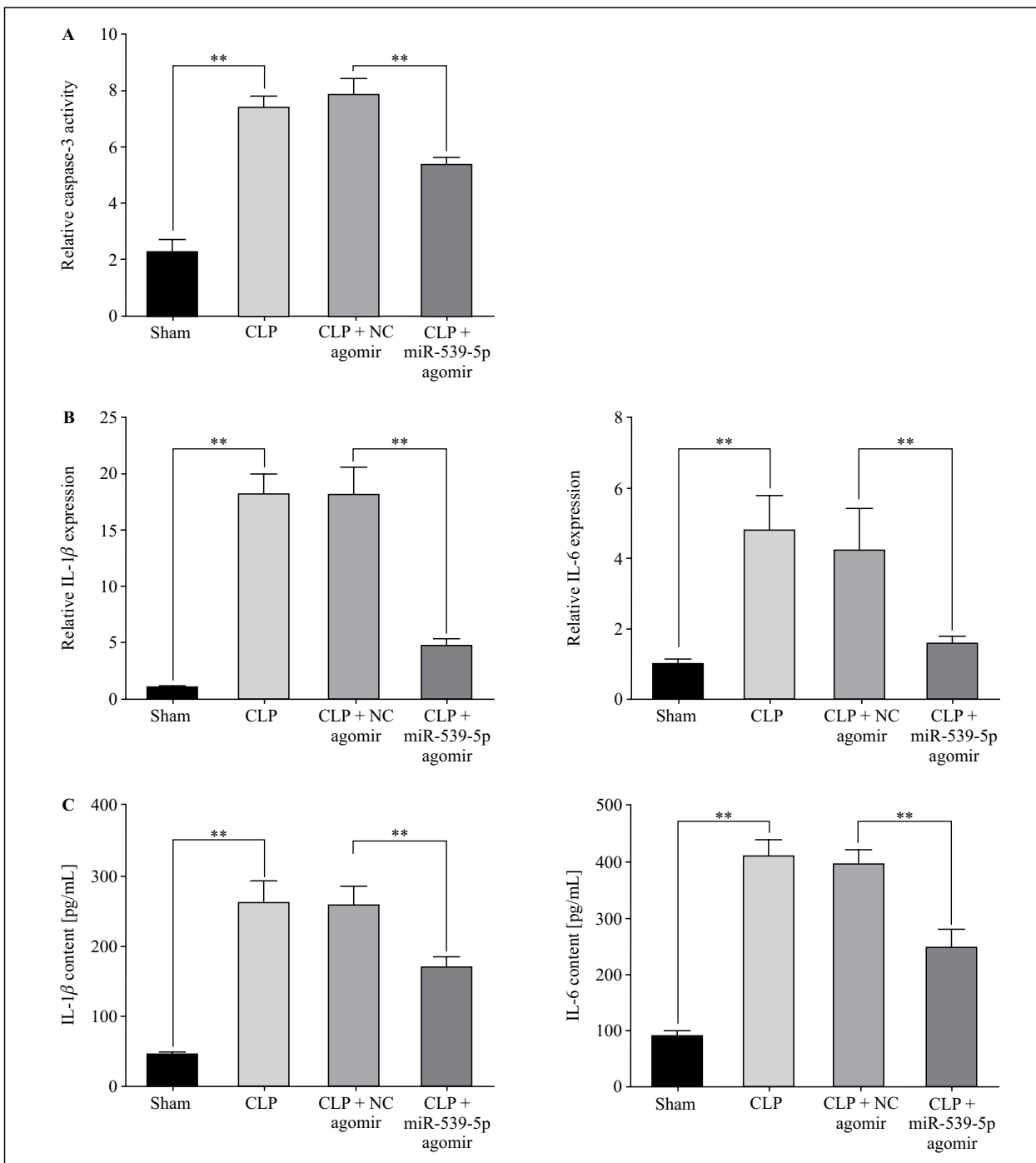


Figure 2. Effect of miR-539-5p overexpression on apoptosis and inflammation in mice lungs following CLP-induced sepsis. **A.** The transcriptional activity of caspase-3 in lung tissues was measured using Caspase-3 Assay Kit. **B–C.** The pulmonary mRNA and protein levels of IL-1 β and IL-6 were examined using qRT-PCR and ELISA, respectively. ***p* < 0.01.

ROCK1, however, increased the activity of caspase-3 back to the level that was shown in control group (Fig. 5C). The production of proinflammatory cytokines in MPVECs was largely inhibited by miR-539-5p overexpression, whereas ROCK1 led to a significant upregulation of IL-1 β and IL-6 at both mRNA

and protein levels (Fig. 5D–E). Moreover, the overexpression of miR-539-5p significantly decreased the apoptosis ratio of MPVECs, whereas the transfection of ROCK1-expressing vectors substantially facilitated MPVECs apoptosis (Fig. 5F). Taken together, these data indicated that miR-539-5p inhibited apoptosis

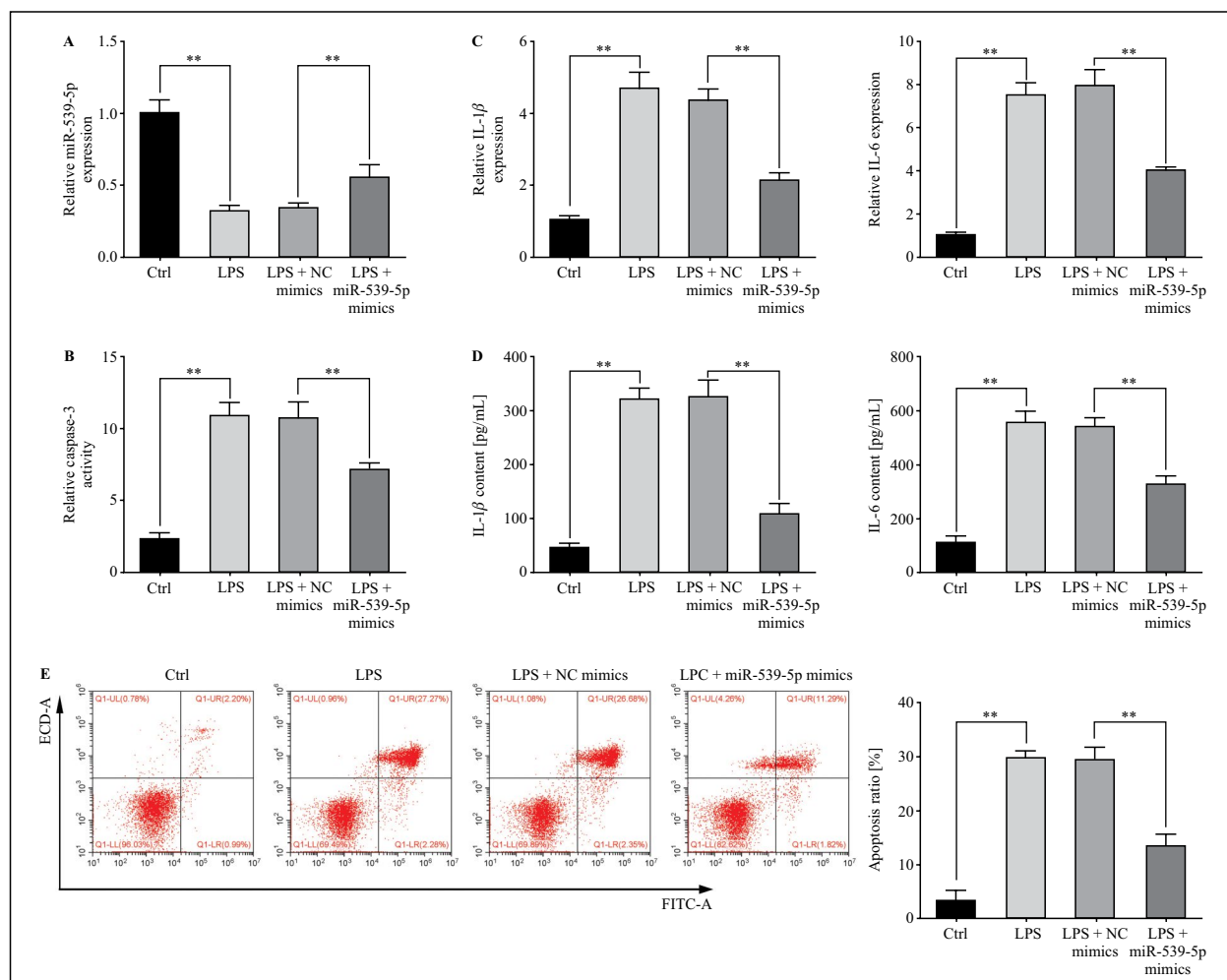


Figure 3. Induction of miR-539-5p affects the expression of apoptosis marker and proinflammatory cytokines in LPS-stimulated primary murine pulmonary microvascular endothelial cells (MPVECs). Isolated MPVECs were divided into four groups: LPS (lipopolysaccharide), LPS + NC mimics, LPS + miR-539-5p mimics and Ctrl. Cells in LPS + NC mimics and LPS + miR-539-5p mimics groups were transfected with control mimics and miR-539-5p mimics, respectively, followed by the stimulation with 1 mg/mL. Cells in LPS group were stimulated with LPS without transfection. Control (Ctrl) cells remained untreated. **A.** Relative expression of miR-539-5p was assessed using qRT-PCR 6 h after the stimulation with lipopolysaccharides (LPS). **B.** The transcriptional activity of caspase-3 was examined 30 min following the treatment. **C–D.** The mRNA and protein levels of IL-1 β and IL-6 were examined using qRT-PCR and ELISA, respectively. **E.** The apoptosis ratio in transfected MPVECs was calculated using flow cytometry analysis. ** $p < 0.01$.

and inflammation in sepsis-induced ALI *via* the suppression of its target gene ROCK1.

Discussion

Sepsis is a leading etiology of ALI that leads to more severe illness and higher mortality rates compared to non-sepsis risk factors [22]. As a syndrome developed from excessive inflammation, ALI affords multiple potential therapeutic targets and signaling pathways [23]. In the present study, we reported for the first time that miR-539-5p mitigated the development

of sepsis-induced ALI both *in vivo* and *in vitro*. The induction of miR-539-5p in septic models decreased the expression of proinflammatory cytokines, IL-1 β and IL-6, and suppressed the transcriptional activity of apoptosis marker, caspase-3. Further investigation revealed that miR-539-5p reduced apoptosis and inflammation in sepsis-induced ALI *via* the negative regulation of its downstream target ROCK1.

Mouse CLP model closely resembles the pathophysiology of human sepsis caused by abdominal perforations and has been extensively used in the research of sepsis-induced organ dysfunction [24]. In

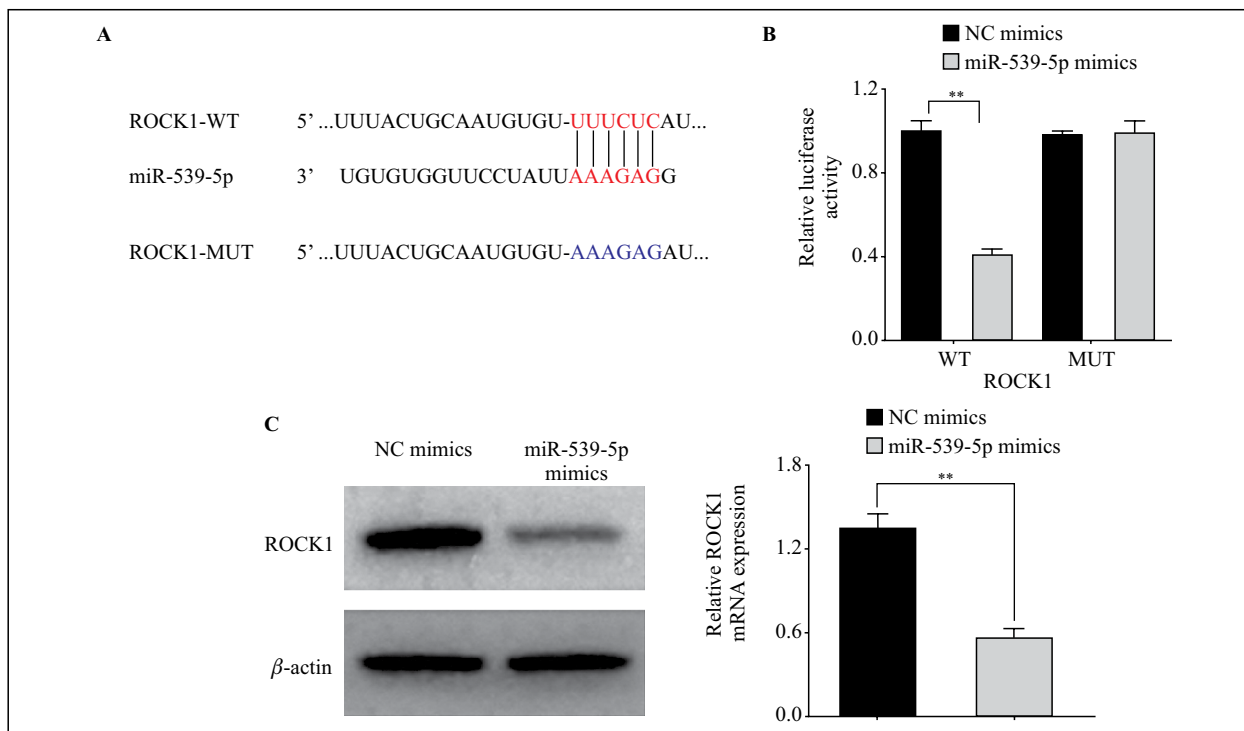


Figure 4. ROCK1 is a direct target of miR-539-5p. ROCK1 was predicted as a direct downstream target of miR-539-5p using TargetScan. **A.** The putative ROCK1 binding site for miR-539-5p (ROCK1-WT) and the designed mutant sequence (ROCK1-MUT) were shown. **B.** HEK-293T cells were co-transfected with NC mimics (or miR-539-5p mimics) and ROCK1-WT (or ROCK1-MUT). The luciferase activity was measuring using dual-luciferase reporter assay. **C.** The expression of ROCK1 in MPVECs transfected with NC mimics and miR-539-5p mimics were examined using Western blot and qRT-PCR.

this study, we successfully established the mouse model of sepsis-induced ALI by performing CLP surgery and showed morphological abnormalities in the lung, including thickened alveolar walls, collapsed alveolar sacs, vascular congestion and hemorrhage in CLP mice as compared to sham-operated group. Enhanced cell apoptosis and the induction of proinflammatory mediators during sepsis play crucial roles in the pathogenesis of ALI [25]. IL-1 β and IL-6 are two proinflammatory cytokines actively secreted in response to the inflammatory cascade in ALI [26, 27]. The inhibition of apoptotic signaling and inflammatory responses might potentially ameliorate sepsis-induced lung damage. The caspase-3 activity is an important marker of cellular apoptosis. Increased activation of caspase-3 has been reported in the animal models of ALI [28, 29]. In the current study, enhanced caspase-3 activity, elevated production of IL-1 β and IL-6, together with the increased apoptosis ratio was observed following CLP operation. LPS is an endotoxin constituting the outer membrane of Gram-negative bacteria, and has been widely used to induce acute lung injury in research [30]. In the *in vitro* model, incubation with LPS led to a significant induction of inflammatory

cytokine levels and apoptosis in MPVECs compared to untreated cells.

The potential involvement of miRNAs in ALI was first shown in a mouse model of LPS-induced lung injury, in which certain types of miRNAs were significantly downregulated and the others were remarkably upregulated or remained unaltered [31]. Further investigations on the role of miRNAs in ALI suggested that miRNAs might regulate the inflammatory and apoptotic pathways during ALI progression by targeting specific molecules or regulating downstream genes [32]. Tuerdi *et al.* reported that the downregulation of miR-155 inhibited lung apoptosis and inflammation, and increased the survival rate in CLP-induced ALI mice by targeting SIRT1 [33]. The depletion of miR-1246 reduced apoptosis, the release of IL-1 β , and neutrophil infiltration in mice with ALI through the repression of its downstream target ACE2 [34]. Xie *et al.* showed significantly reduced expression of miR-127 during lung injury *in vivo*, while the administration of miR-127 probes attenuated pulmonary inflammation through the regulation of CD46 in macrophages [35]. In another animal study, the upregulation of miR146a suppressed the secretion of TNF- α , IL-6,

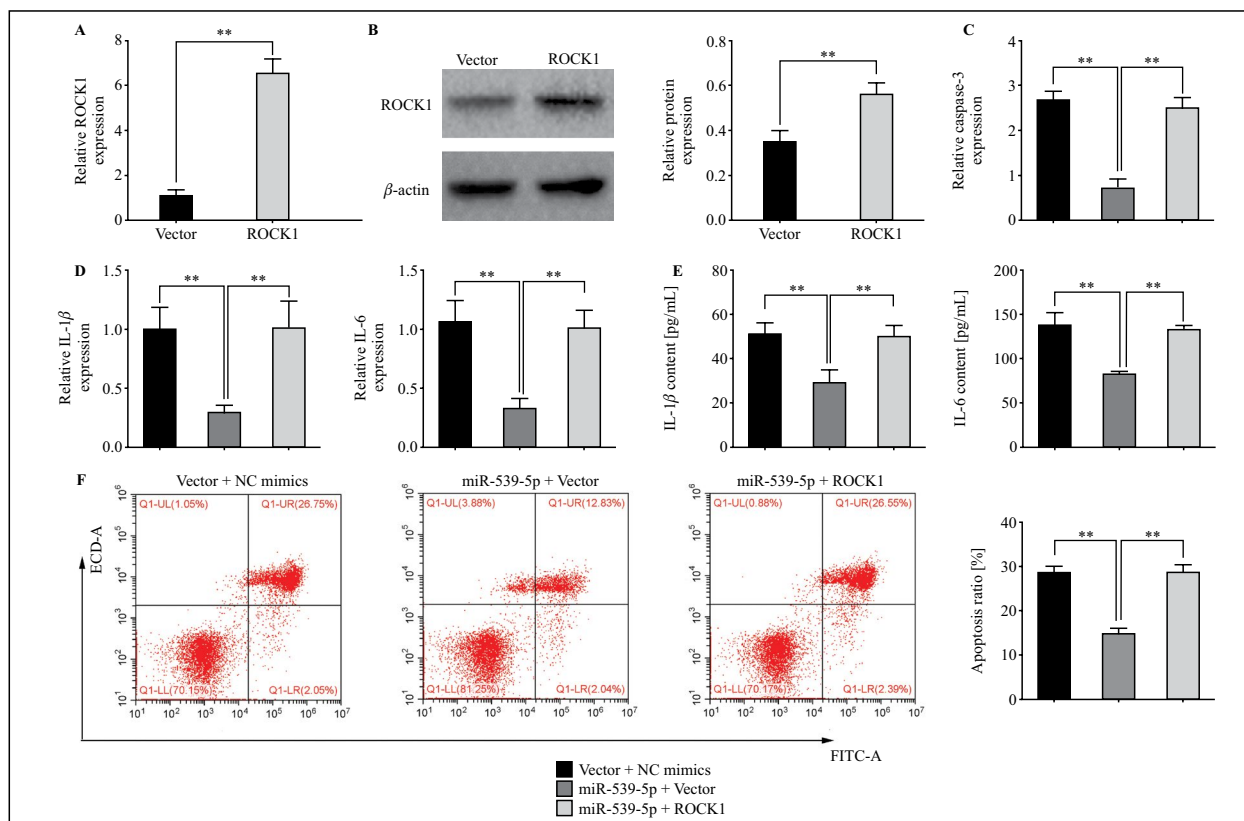


Figure 5. MiR-539-5p mediated apoptosis and inflammation via regulating ROCK1. MPVECs were divided into three groups: miR-539-5p + Vector, miR-539-5p + ROCK1 and Vector + NC mimics. In miR-539-5p + Vector and miR-539-5p + ROCK1 groups, MPVECs were co-transfected with miR-539-5p mimics and lentiviral vector expressing ROCK1 (or empty lentiviral vector) 24 h before LPS stimulation. MPVECs in Vector + NC mimics group were co-transfected with empty lentiviral vector and control mimics. **A–B.** To evaluate the transfection efficacy, the mRNA and protein levels of ROCK1 in miR-539-5p + Vector and miR-539-5p + ROCK1 groups were analyzed using qRT-PCR and Western blot. **C.** The transcriptional activity of caspase-3 was examined 30 min post-stimulation. **D–E.** The mRNA and protein levels of IL-1 β and IL-6 were determined using qRT-PCR and ELISA, respectively. **F.** The apoptosis ratio in transfected MPVECs was calculated using flow cytometry analysis. ** $p < 0.01$.

and IL-1 β in LPS-induced ALI model via the inhibition of IRAK-1 and TRAF-6 [36]. In our study, we showed that the level of miR-539-5p was significantly downregulated in CLP-operated mice compared to the sham group. The delivery of miR-539-5p mimics prior to CLP surgery efficiently alleviated sepsis-induced pulmonary injury, reduced caspase-3 activity and apoptosis, suppressed the induction of inflammatory cytokines IL-1 β and IL-6. The anti-apoptotic and anti-inflammatory effect of miR-539-5p were also shown in LPS-treated MPVECs.

ROCK1 has been predicted and confirmed as a direct downstream target of miR-539-5p in our study. A previous study in CLP rat model showed that the

activation of ROCK1 was involved in the pathogenesis of sepsis-induced ALI with a potential mechanism related to oxidative stress and apoptosis [37]. Here, by enhancing the expression of ROCK1 in MPVECs, the beneficial effect of miR-539-5p in ALI-associated apoptosis and inflammation was significantly reversed. It indicated that miR-539-5p ameliorated sepsis-induced ALI by repressing its downstream target ROCK1.

In conclusion, miR-539-5p alleviated sepsis-induced apoptosis and proinflammatory cytokine production during ALI by downregulating the expression of ROCK1. This study highlighted the potential of miR-539-5p as a therapeutic target for the management of sepsis-induced ALI.

Competing interests

The authors declare that they have no competing interests, and all authors should confirm its accuracy.

Availability of data and materials

All data generated or analyzed during this study are included in this published article.

Authors' contributions

LM and CHW conceived and designed the experiments, HHC analyzed and interpreted the results of the experiments, LTJ performed the experiments.

Ethics approval and consent to participate

The animal use protocol listed below has been reviewed and approved by the Animal Ethical and Welfare Committee of Hubei Provincial Hospital.

Patient consent for publication

Not Applicable.

Informed consent

Written informed consent was obtained from a legally authorized representative(s) for anonymized patient information to be published in this article.

References

- Sagy M, Al-Qaqa Y, Kim P. Definitions and pathophysiology of sepsis. *Curr Probl Pediatr Adolesc Health Care*. 2013; 43(10): 260–263, doi: [10.1016/j.cppeds.2013.10.001](https://doi.org/10.1016/j.cppeds.2013.10.001), indexed in Pubmed: [24295606](https://pubmed.ncbi.nlm.nih.gov/24295606/).
- Gando S. Microvascular thrombosis and multiple organ dysfunction syndrome. *Crit Care Med*. 2010; 38(2 Suppl): S35–S42, doi: [10.1097/CCM.0b013e3181c9e31d](https://doi.org/10.1097/CCM.0b013e3181c9e31d), indexed in Pubmed: [20083912](https://pubmed.ncbi.nlm.nih.gov/20083912/).
- Levitt JE, Matthay MA. The utility of clinical predictors of acute lung injury: towards prevention and earlier recognition. *Expert Rev Respir Med*. 2010; 4(6): 785–797, doi: [10.1586/ers.10.78](https://doi.org/10.1586/ers.10.78), indexed in Pubmed: [21128753](https://pubmed.ncbi.nlm.nih.gov/21128753/).
- Johnson ER, Matthay MA. Acute lung injury: epidemiology, pathogenesis, and treatment. *J Aerosol Med Pulm Drug Deliv*. 2010; 23(4): 243–252, doi: [10.1089/jamp.2009.0775](https://doi.org/10.1089/jamp.2009.0775), indexed in Pubmed: [20073554](https://pubmed.ncbi.nlm.nih.gov/20073554/).
- Levitt JE, Matthay MA. Clinical review: Early treatment of acute lung injury—paradigm shift toward prevention and treatment prior to respiratory failure. *Crit Care*. 2012; 16(3): 223, doi: [10.1186/cc11144](https://doi.org/10.1186/cc11144), indexed in Pubmed: [22713281](https://pubmed.ncbi.nlm.nih.gov/22713281/).
- Park WY, Goodman RB, Steinberg KP, et al. Cytokine balance in the lungs of patients with acute respiratory distress syndrome. *Am J Respir Crit Care Med*. 2001; 164(10 Pt 1): 1896–1903, doi: [10.1164/ajrccm.164.10.2104013](https://doi.org/10.1164/ajrccm.164.10.2104013), indexed in Pubmed: [11734443](https://pubmed.ncbi.nlm.nih.gov/11734443/).
- Goodman RB, Strieter RM, Martin DP, et al. Inflammatory cytokines in patients with persistence of the acute respiratory distress syndrome. *Am J Respir Crit Care Med*. 1996; 154(3 Pt 1): 602–611, doi: [10.1164/ajrccm.154.3.8810593](https://doi.org/10.1164/ajrccm.154.3.8810593), indexed in Pubmed: [8810593](https://pubmed.ncbi.nlm.nih.gov/8810593/).
- Martin TR, Nakamura M, Matute-Bello G. The role of apoptosis in acute lung injury. *Crit Care Med*. 2003; 31(4 Suppl): S184–S188, doi: [10.1097/01.CCM.0000057841.33876.B1](https://doi.org/10.1097/01.CCM.0000057841.33876.B1), indexed in Pubmed: [12682438](https://pubmed.ncbi.nlm.nih.gov/12682438/).
- Perl M, Chung CS, Perl U, et al. Fas-induced pulmonary apoptosis and inflammation during indirect acute lung injury. *Am J Respir Crit Care Med*. 2007; 176(6): 591–601, doi: [10.1164/rccm.200611-1743OC](https://doi.org/10.1164/rccm.200611-1743OC), indexed in Pubmed: [17600273](https://pubmed.ncbi.nlm.nih.gov/17600273/).
- Kitamura Y, Hashimoto S, Mizuta N, et al. Fas/FasL-dependent apoptosis of alveolar cells after lipopolysaccharide-induced lung injury in mice. *Am J Respir Crit Care Med*. 2001; 163(3 Pt 1): 762–769, doi: [10.1164/ajrccm.163.3.2003065](https://doi.org/10.1164/ajrccm.163.3.2003065), indexed in Pubmed: [11254536](https://pubmed.ncbi.nlm.nih.gov/11254536/).
- Kingsley SM, Bhat BV. Role of microRNAs in sepsis. *Inflamm Res*. 2017; 66(7): 553–569, doi: [10.1007/s00011-017-1031-9](https://doi.org/10.1007/s00011-017-1031-9), indexed in Pubmed: [28258291](https://pubmed.ncbi.nlm.nih.gov/28258291/).
- Adameova AD, Bhullar SK, Elimban V, et al. Activation of α -adrenoceptors may not be involved in arrhythmogenesis in ischemic heart disease. *Rev Cardiovasc Med*. 2018; 19(3): 97–101, doi: [10.31083/j.rcm.2018.03.3181](https://doi.org/10.31083/j.rcm.2018.03.3181), indexed in Pubmed: [31054558](https://pubmed.ncbi.nlm.nih.gov/31054558/).
- Yang Q, Zhang D, Li Ya, et al. Paclitaxel alleviated liver injury of septic mice by alleviating inflammatory response via microRNA-27a/TAB3/NF- κ B signaling pathway. *Biomed Pharmacother*. 2018; 97: 1424–1433, doi: [10.1016/j.biopha.2017.11.003](https://doi.org/10.1016/j.biopha.2017.11.003), indexed in Pubmed: [29156532](https://pubmed.ncbi.nlm.nih.gov/29156532/).
- Feng Y, Wang J, Yuan Y, et al. miR-539-5p inhibits experimental choroidal neovascularization by targeting CXCR7. *FASEB J*. 2018; 32(3): 1626–1639, doi: [10.1096/fj.201700640R](https://doi.org/10.1096/fj.201700640R), indexed in Pubmed: [29146732](https://pubmed.ncbi.nlm.nih.gov/29146732/).
- Hu L, Liu Y, Wang B, et al. MiR-539-5p negatively regulates migration of rMSCs induced by Bushen Huoxue decoction through targeting Wnt5a. *Int J Med Sci*. 2019; 16(7): 998–1006, doi: [10.7150/ijms.33437](https://doi.org/10.7150/ijms.33437), indexed in Pubmed: [31341413](https://pubmed.ncbi.nlm.nih.gov/31341413/).
- National Research Council Institute for Laboratory Animal R. Guide for the Care and Use of Laboratory Animals. Washington (DC): National Academies Press (US), 1996.
- Matsuda N, Hattori Y, Jesmin S, et al. Nuclear factor-kappaB decoy oligodeoxynucleotides prevent acute lung injury in mice with cecal ligation and puncture-induced sepsis. *Mol Pharmacol*. 2005; 67(4): 1018–1025, doi: [10.1124/mol.104.005926](https://doi.org/10.1124/mol.104.005926), indexed in Pubmed: [15576632](https://pubmed.ncbi.nlm.nih.gov/15576632/).
- Ruiz S, Vardon-Bounes F, Merlet-Dupuy V, et al. Sepsis modeling in mice: ligation length is a major severity factor in cecal ligation and puncture. *Intensive Care Med Exp*. 2016; 4(1): 22, doi: [10.1186/s40635-016-0096-z](https://doi.org/10.1186/s40635-016-0096-z), indexed in Pubmed: [27430881](https://pubmed.ncbi.nlm.nih.gov/27430881/).
- Morishita Y, Imai T, Yoshizawa H, et al. Delivery of microRNA-146a with polyethylenimine nanoparticles inhibits renal fibrosis in vivo. *Int J Nanomedicine*. 2015; 10: 3475–3488, doi: [10.2147/IJN.S82587](https://doi.org/10.2147/IJN.S82587), indexed in Pubmed: [25999712](https://pubmed.ncbi.nlm.nih.gov/25999712/).
- Matute-Bello G, Downey G, Moore BB, et al. Acute Lung Injury in Animals Study Group. An official American Thoracic Society workshop report: features and measurements of experimental acute lung injury in animals. *Am J Respir Cell Mol Biol*. 2011; 44(5): 725–738, doi: [10.1165/rccb.2009-0210ST](https://doi.org/10.1165/rccb.2009-0210ST), indexed in Pubmed: [21531958](https://pubmed.ncbi.nlm.nih.gov/21531958/).
- Hebbel RP, Vercellotti GM, Pace BS, et al. The HDAC inhibitors trichostatin A and suberoylanilide hydroxamic

- acid exhibit multiple modalities of benefit for the vascular pathobiology of sickle transgenic mice. *Blood*. 2010; 115(12): 2483–2490, doi: [10.1182/blood-2009-02-204990](https://doi.org/10.1182/blood-2009-02-204990), indexed in Pubmed: [20053759](https://pubmed.ncbi.nlm.nih.gov/20053759/).
22. Sevransky JE, Martin GS, Shanholtz C, et al. Mortality in sepsis versus non-sepsis induced acute lung injury. *Crit Care*. 2009; 13(5): R150, doi: [10.1186/cc8048](https://doi.org/10.1186/cc8048), indexed in Pubmed: [19758459](https://pubmed.ncbi.nlm.nih.gov/19758459/).
 23. Sweeney RM, Griffiths M, McAuley D. Treatment of acute lung injury: current and emerging pharmacological therapies. *Semin Respir Crit Care Med*. 2013; 34(4): 487–498, doi: [10.1055/s-0033-1351119](https://doi.org/10.1055/s-0033-1351119), indexed in Pubmed: [23934717](https://pubmed.ncbi.nlm.nih.gov/23934717/).
 24. Rittirsch D, Hoesel LM, Ward PA. The disconnect between animal models of sepsis and human sepsis. *J Leukoc Biol*. 2007; 81(1): 137–143, doi: [10.1189/jlb.0806542](https://doi.org/10.1189/jlb.0806542), indexed in Pubmed: [17020929](https://pubmed.ncbi.nlm.nih.gov/17020929/).
 25. Chopra M, Reuben JS, Sharma AC. Acute lung injury: apoptosis and signaling mechanisms. *Exp Biol Med (Maywood)*. 2009; 234(4): 361–371, doi: [10.3181/0811-MR-318](https://doi.org/10.3181/0811-MR-318), indexed in Pubmed: [19176873](https://pubmed.ncbi.nlm.nih.gov/19176873/).
 26. Ganter MT, Roux J, Miyazawa B, et al. Interleukin-1beta causes acute lung injury via alphavbeta5 and alphavbeta6 integrin-dependent mechanisms. *Circ Res*. 2008; 102(7): 804–812, doi: [10.1161/CIRCRESAHA.107.161067](https://doi.org/10.1161/CIRCRESAHA.107.161067), indexed in Pubmed: [18276918](https://pubmed.ncbi.nlm.nih.gov/18276918/).
 27. Cross LJ, Matthay MA. Biomarkers in acute lung injury: insights into the pathogenesis of acute lung injury. *Crit Care Clin*. 2011; 27(2): 355–377, doi: [10.1016/j.ccc.2010.12.005](https://doi.org/10.1016/j.ccc.2010.12.005), indexed in Pubmed: [21440206](https://pubmed.ncbi.nlm.nih.gov/21440206/).
 28. Fielhaber JA, Carroll SF, Dydensborg AB, et al. Inhibition of mammalian target of rapamycin augments lipopolysaccharide-induced lung injury and apoptosis. *J Immunol*. 2012; 188(9): 4535–4542, doi: [10.4049/jimmunol.1003655](https://doi.org/10.4049/jimmunol.1003655), indexed in Pubmed: [22450807](https://pubmed.ncbi.nlm.nih.gov/22450807/).
 29. Wang L, Ye Y, Su HB, et al. The anesthetic agent sevoflurane attenuates pulmonary acute lung injury by modulating apoptotic pathways. *Braz J Med Biol Res*. 2017; 50(3): e5747, doi: [10.1590/1414-431X20165747](https://doi.org/10.1590/1414-431X20165747), indexed in Pubmed: [28225890](https://pubmed.ncbi.nlm.nih.gov/28225890/).
 30. Jeyaseelan S, Chu HW, Young SK, et al. Transcriptional profiling of lipopolysaccharide-induced acute lung injury. *Infect Immun*. 2004; 72(12): 7247–7256, doi: [10.1128/IAI.72.12.7247-7256.2004](https://doi.org/10.1128/IAI.72.12.7247-7256.2004), indexed in Pubmed: [15557650](https://pubmed.ncbi.nlm.nih.gov/15557650/).
 31. Cai ZG, Zhang SM, Zhang Y, et al. MicroRNAs are dynamically regulated and play an important role in LPS-induced lung injury. *Can J Physiol Pharmacol*. 2012; 90(1): 37–43, doi: [10.1139/y11-095](https://doi.org/10.1139/y11-095), indexed in Pubmed: [22185353](https://pubmed.ncbi.nlm.nih.gov/22185353/).
 32. Cao Y, Lyu YI, Tang J, et al. MicroRNAs: Novel regulatory molecules in acute lung injury/acute respiratory distress syndrome. *Biomed Rep*. 2016; 4(5): 523–527, doi: [10.3892/br.2016.620](https://doi.org/10.3892/br.2016.620), indexed in Pubmed: [27123242](https://pubmed.ncbi.nlm.nih.gov/27123242/).
 33. Liu Y, Guan H, Zhang JL, et al. Acute downregulation of miR-199a attenuates sepsis-induced acute lung injury by targeting SIRT1. *Am J Physiol Cell Physiol*. 2018; 314(4): C449–C455, doi: [10.1152/ajpcell.00173.2017](https://doi.org/10.1152/ajpcell.00173.2017), indexed in Pubmed: [29351405](https://pubmed.ncbi.nlm.nih.gov/29351405/).
 34. Fang Y, Gao F, Hao J, et al. microRNA-1246 mediates lipopolysaccharide-induced pulmonary endothelial cell apoptosis and acute lung injury by targeting angiotensin-converting enzyme 2. *Am J Transl Res*. 2017; 9(3): 1287–1296, indexed in Pubmed: [28386354](https://pubmed.ncbi.nlm.nih.gov/28386354/).
 35. Xie T, Liang J, Liu N, et al. MicroRNA-127 inhibits lung inflammation by targeting IgG Fcγ receptor I. *J Immunol*. 2012; 188(5): 2437–2444, doi: [10.4049/jimmunol.1101070](https://doi.org/10.4049/jimmunol.1101070), indexed in Pubmed: [22287715](https://pubmed.ncbi.nlm.nih.gov/22287715/).
 36. Zeng Z, Gong H, Li Y, et al. Upregulation of miR-146a contributes to the suppression of inflammatory responses in LPS-induced acute lung injury. *Exp Lung Res*. 2013; 39(7): 275–282, doi: [10.3109/01902148.2013.808285](https://doi.org/10.3109/01902148.2013.808285), indexed in Pubmed: [23848342](https://pubmed.ncbi.nlm.nih.gov/23848342/).
 37. Cinel I, Ark M, Dellinger P, et al. Involvement of Rho kinase (ROCK) in sepsis-induced acute lung injury. *J Thorac Dis*. 2012; 4(1): 30–39, doi: [10.3978/j.issn.2072-1439.2010.08.04](https://doi.org/10.3978/j.issn.2072-1439.2010.08.04), indexed in Pubmed: [22295165](https://pubmed.ncbi.nlm.nih.gov/22295165/).

Submitted: 27 September, 2019

Accepted after reviews: 14 November, 2019

Available as AoP: 11 December, 2019

Increased expression of CART, nNOS, VIP, PACAP, SP and GAL in enteric neurons of the porcine stomach prepyloric region following hydrochloric acid infusion

Jaroslaw Calka

Department of Clinical Physiology, Faculty of Veterinary Medicine,
University of Warmia and Mazury, Olsztyn, Poland

Abstract

Introduction. Stomach hyperacidity leads to damage of the mucus/bicarbonate barrier, ulcerations and the development of stomach cancer. Key regulators of the mucosal barrier/luminal acid balance are neurotransmitters secreted by intramural neurons. The aim of the current study was to determine the expression of gastric neuropeptides and nNOS in the porcine stomach following hydrochloric acid instillation. We report on increased expression of enteric neurotransmitters involved in adaptive reaction to an experimentally-induced hyperacidity state.

Material and methods. The investigation was conducted on eight 12–18 kg pigs. The influence of intragastric infusion of hydrochloric acid on the expression of cocaine- and amphetamine-regulated transcript peptide (CART), neuronal nitric oxide synthase (nNOS), vasoactive intestinal polypeptide (VIP), pituitary adenylate cyclase-activating peptide (PACAP), substance P (SP) and galanin (GAL) in the submucous and myenteric gastric neurons of the pig has been studied with double immunofluorescence.

Results. A mimicked hyperacidity state significantly increased the proportion of enteric neurons immunoreactive to CART, nNOS, VIP, PACAP, SP and GAL in the submucous gastric neurons. In the myenteric plexus, a significant increase of the number of VIP-, CART- and GAL-immunoreactive (IR) neurons was found. Similarly, the percentage of myenteric nNOS-IR and PACAP-IR neurons tended to increase, while the fraction of SP-IR cells did not change.

Conclusions. Stomach hyperacidity modifies the expression of the studied neurotransmitters in a specific way depending on the location of the neurons in particular plexuses of the stomach. Increased numbers of neurons expressing CART, nNOS, VIP, PACAP, SP and GAL clearly indicate their regulatory engagement in the restoration of the physiological gastric balance following hyperacidity. (*Folia Histochemica et Cytobiologica* 2019, Vol. 57, No. 4, 179–187)

Key words: pig; stomach; hyperacidity; enteric nervous system; neuropeptides; IHC

Introduction

Stomach digestive function is based on the secretion of gastric juice, whose main ingredients are hydrochloric acid (HCl), pepsinogen, mucus and HCO_3^- ions. HCl and the proteolytic enzyme pepsin participate in the

digestion of proteins, while mucus and HCO_3^- protect the mucosal lining against acid-pepsin digestion [1].

Gastric acid secretion is stimulated by various neuronal (vagal, enteric), paracrine (histamine) and hormonal (gastrin) factors, while somatostatin, glucagon-like peptide-1, cholecystokinin and atrial natriuretic peptide reduce secretory stomach activity [2]. Gastric hyperacidity states increase the risk of numerous gastrointestinal disorders and increase morbidity and mortality related to those pathologies [3–5]. Excessive secretion of gastric juice may cause destruction of the mucous protection barrier, the development of erosions, formation of ulcers ac-

Correspondence address: Prof. Jaroslaw Calka
Department of Clinical Physiology,
Faculty of Veterinary Medicine,
University of Warmia and Mazury,
Oczapowskiego 13, 10–718 Olsztyn, Poland
e-mail: calkaj@uwm.edu.pl

accompanied by inflammatory state [6, 7] and, finally, the development of cancer [8]. Based on previous observations, this harmful environment might trigger adaptive reaction of the stomach intramural neurons, whose nature, due to a lack of adequate data, remains unclear [9].

Intramural gastric neurons constitute a local emergency system that is called into operation when the gastric mucosa is endangered by acid or other harmful stimuli [10]. Among the active factors are neurotransmitters synthesized and released by enteric neurons [11]. Identification of the hyperacidity-induced neuroactive substances constitutes the first indicator of their possible engagement in the gastric mucosal repair or degradation process. Although available reports implicate certain neurotransmitters like cocaine- and amphetamine-regulated transcript peptide (CART) [12, 13], nitric oxide (NO) [14, 15], VIP — vasoactive intestinal polypeptide [5], pituitary adenylate cyclase-activating peptide (PACAP) [16], substance P (SP) [10, 17, 18], galanin (GAL) [2, 19] in the maintenance of the luminal mucus-hydrochloric acid equilibrium, the specific neuronal populations that synthesize and release those substances still remain obscure.

In the pig, the anatomy of the enteric nervous system depends on the segment of digestive tract [19]. In the stomach, it is composed of two intramural plexuses: the myenteric plexus and the submucous plexus. It is widely accepted that myenteric neurons are responsible for the control of stomach and gut motor function, whereas submucous neurons mainly regulate mucosal secretion [20–22]. It has also been reported that local gastric neurons respond with structural, functional and neurochemical changes to inflammatory processes, bacterial infections, toxins and intestinal diseases [23]. Consistently, the enteric neurons are known to be highly plastic in their response to inflammation [24, 25]. This adaptive reaction comprises both up and down adjustment of transmitter expression and the induction of new genes that induce *de novo* expression of neurotransmitters formerly absent in the enteric neurons. The adaptive response occurs to promote enteric neurons to survive pathological conditions, but also to facilitate the healing process of the inflamed part of the gastrointestinal tract [26].

Thus, the influence of intragastric HCl instillation on the expression of CART-, neuronal NOS-, VIP-, PACAP-, SP- and GAL- immunoreactivity in the porcine stomach intrinsic neurons was studied. The pig, like humans [27, 28], is a species particularly susceptible to ulcer formation. We have chosen the stomach prepyloric region since this area is pathognomonic for the location of peptic ulcers which, when

localized here, may alter gastric emptying [29]. Moreover, selection of the pig as an experimental animal species is based on close anatomical and physiological resemblance and human-like sensitivity of this species to stressful conditions [30].

Materials and methods

The present investigation was conducted on eight immature female pigs of the Large White Polish breed (12–18 kg *b.w.*, approximately 8 weeks old), which were kept in standard laboratory conditions during the experiment. Animals were purchased from Production and Testing Plant “Balcyny” in Balcyny. All experimental actions were conducted in compliance with the instructions of the Local Ethical Committee in Olsztyn, decision number 05/2010.

Pigs were randomly divided into two groups: a control (group C; $n = 4$) and an experimental group (HCL group, $n = 4$). Animals of the experimental group were pre-treated with atropine (Polfa, Warszawa, Poland, 0.4 mg/kg, *s.c.*) and propionyl promazine (Stresnil, Janssen, Beerse, Belgium, 0.8 mg/kg, *i.m.*) 15 min. before the application of the main anesthetic — sodium thiopental (Thiopental; Sandoz, Kundl, Austria; 20 mg/kg *i.v.*). Following this, a 0.25 M aqueous solution of hydrochloric acid with a dose of 5 ml/kg of body weight was administered intragastrically using a stomach tube. On the first day and on the seventh day of experiment, endoscopic examinations (using a video-endoscope Olympus GIF 145 with working length 1030 mm and diameter 9.8 mm) were performed to confirm inflammatory changes caused by HCl treatment within gastric mucosal layer. These examinations were conducted under general anesthesia (as mentioned above). Immediately after gastroscopy, animals of both groups were euthanized by an overdose of sodium thiopental. On the same day, the control animals were also anaesthetized, and then euthanized by an overdose of sodium thiopental. Afterwards, all animals (C and HCL groups) were perfused transcardially with 4% buffered paraformaldehyde (pH 7.4) prepared *ex tempore*.

Stomachs were collected from all animals and were then fixed in 4% paraformaldehyde for 20 min, rinsed in a 0.1 M phosphate buffer solution, pH 7.4, for 72 h at 4°C and then kept at 4°C in a buffered 18% sucrose solution. Next, tissue samples of the prepyloric region of the stomach were collected. The sample was taken from the area located 5 cm from the pylorus. Tissue specimens were cut with a cryostat at -22°C (Microm HM-525, Microm International GmbH, Walldorf, Germany) into 14- μ m-thick sections. To preclude double counting, the analysis covered only neurons with well visible nucleus, which were located at least 100 μ m apart from each other.

Sections were processed for the routine double labelling immunofluorescence method, using primary antibodies against the particular active substances studied. Briefly, after

Table 1. Primary and secondary antibodies used in the study

Antigen	Species of origin	Code	Dilution	Supplier
PRIMARY ANTIBODIES				
PGP-9,5	Mouse	7863-2004	1:500	AbDserotec
SP	Rat	8450-0505	1:150	AbDserotec
CART	Rabbit	MAB 163	1:8000	R&D
nNOS	Rabbit	AB5380	1:3000	Chemicon
VIP	Rabbit	VA 1285	1:2000	Biogene
GAL	Rabbit	AB2233	1:2000	Milipore
PACAP	Guinea pig	T-5039	1:2000	PENINSUL
SECONDARY ANTIBODIES				
Alexa Fluor 488	Donkey Anti-Mouse	A21202	1:1000	Life Technologies
Alexa Fluor 546	Donkey Anti-Rabbit	A11010	1:1000	Life Technologies
Alexa Fluor 546	Donkey Anti-Rat	A11081	1:1000	Invitrogen
Alexa Fluor 546	Donkey Anti- Guinea pig	A11074	1:1000	Invitrogen

CART — cocaine- and amphetamine-regulated transcript; GAL — galanin; nNOS — neuronal nitric oxide synthase; PACAP — pituitary adenylate cyclase-activating polypeptide; PGP 9.5 — protein gene product (pan-neuronal marker); SP — substance P; VIP — vasoactive intestinal peptide.

air-drying at room temperature (RT) for 45 min., sections were incubated with a blocking solution containing 10% of normal goat serum, 0.1% bovine serum albumin, 0.01% NaN₃, Triton x-100 and thimerosal in phosphate-buffered saline (PBS) (all these reagents purchased from Sigma, Aldrich, Poznan, Poland) for 1 h at RT. They were then incubated (overnight; RT, in a humid chamber) with a combination of antibodies against protein gene-product (PGP-9.5) with substance P or cocaine- and amphetamine- regulated transcript peptide, pituitary adenylate cyclase-activating polypeptide, galanin, vasoactive intestinal polypeptide or neuronal isoform of nitric oxide synthase. Primary antibodies bound to appropriate antigens were visualized by incubation (1 h, RT) with species-specific secondary antisera conjugated to Alexa Fluor 546 and Alexa Fluor 488 (1 h, RT). Each step of immunolabeling was followed by rinsing of the sections with PBS (3 × 10 min, pH 7.4). The specifications of antibodies are detailed in Table 1. Standard controls, *i.e.* pre-absorption of the neuropeptide antibodies with appropriate antigens for 18 h at 37°C, omission and replacement of primary antibodies by non-immune sera were performed to test the antibodies and specificity of the method.

The labeled sections were analyzed using an Olympus BX51 (Olympus, Tokyo, Japan) fluorescence microscope equipped with epi-illumination and appropriate filter sets. Expression of each studied bioactive substance was analyzed in at least 500 PGP-positive neural cells. Finally, the obtained data were pooled, expressed as means ± SEM and statistically analyzed using GraphPad Prism 5 software (GraphPad Software, San Diego, CA, USA). The differences were considered statistically significant at $P \leq 0.05$.

Results

Microscopic examination of enteric innervation of the stomach prepyloric region in physiological conditions revealed the expression of CART, nNOS, VIP, PACAP, SP and GAL in neurons of the submucous as well as the myenteric plexus (Figs. 1 and 2, Table 2). In the submucous plexus, intragastric HCl instillation resulted in a significant increase in the proportion of neurons expressing CART, nNOS, VIP, PACAP, SP and GAL. In the neurons of the myenteric plexus, a significant increase in the numbers of VIP-, CART- and GAL-immunopositive cells was found. The percentage of nNOS- and PACAP-positive neurons increased insignificantly, while the number of SP-immunoreactive cells did not changed.

Detailed exploration of the CART expression revealed that in the submucous plexus CART was found in 7% of control neurons and 24% of neurons following HCl treatment. In the myenteric plexus, CART-immunoreactive (-IR) cells constituted 33% of control neurons and 51% of the immunoreactive cells after HCl application.

In the submucous plexus of the control group, nNOS was expressed in 4% of neurons, while in hyperacidic animals it was expressed in 20% of the PGP-9.5-IR cells. Myenteric plexus showed nNOS in 20% of the gastric control neurons and 27% cells of the experimental animals.

Hyperacidic conditions in the submucous plexus caused an increase in the ratio of VIP-IR neurons from 2% in controls to 11% in experimental pigs,

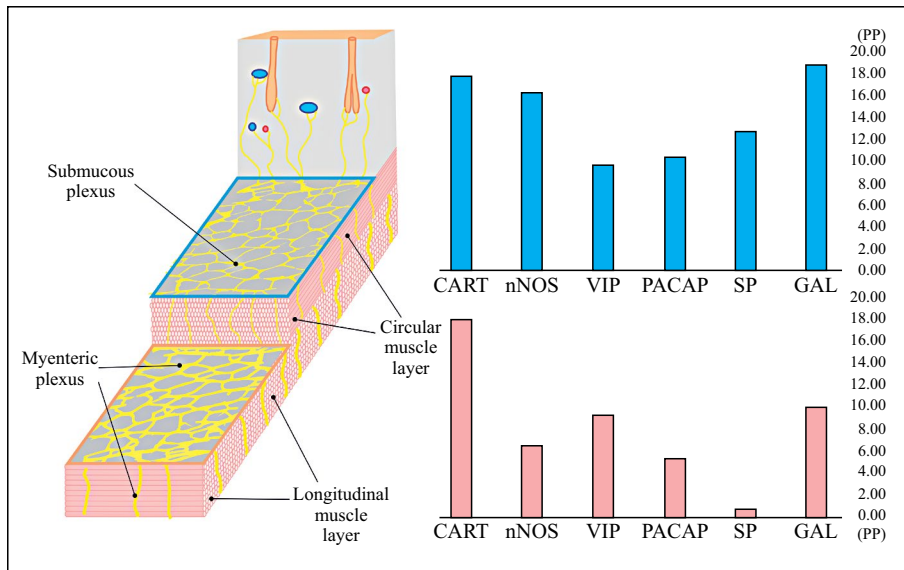


Figure 1. Diagram showing percent point (pp) increase of the number of CART-, nNOS-, VIP-, PACAP-, SP- and GAL-immunoreactive neurons in submucous plexus (blue) and myenteric plexus (orange) in the porcine prepyloric region following hydrochloric acid intragastric instillation to pigs. For abbreviations: see the description of Table 1.

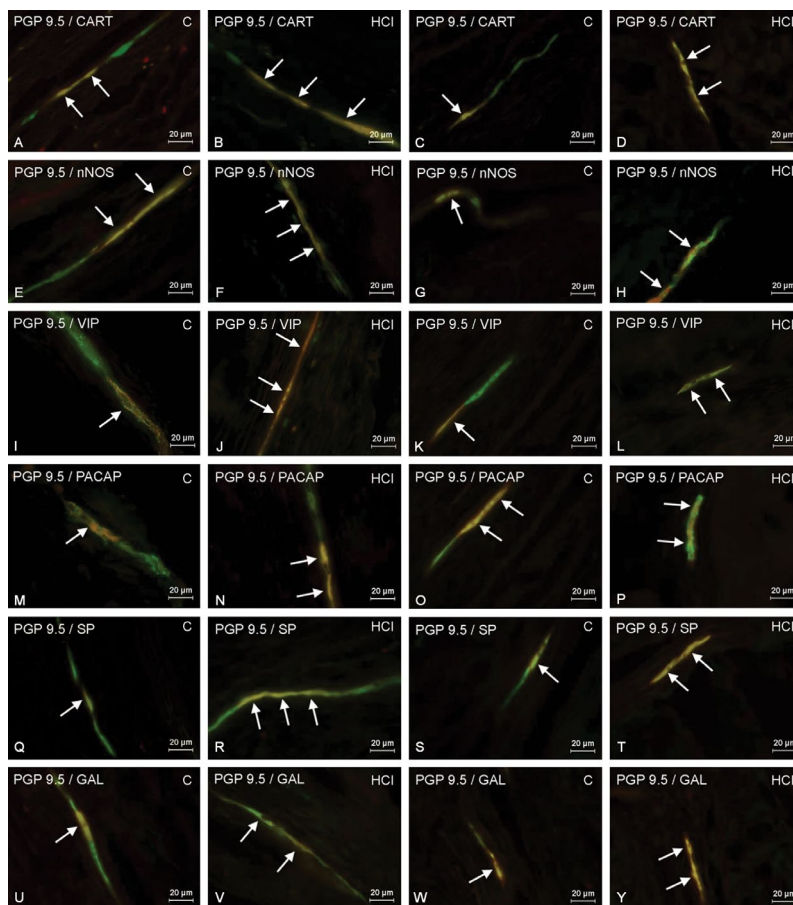


Figure 2. The immunoreactivity of the studied neuropeptides in the submucous plexus (A, B, E, F, I, J, M, N, Q, R, U, V) and myenteric plexus (C, D, G, H, K, L, O, P, S, T, W, Y) co-localized with protein gene product 9.5 (PGP 9.5) in the stomach prepyloric region in control (C) and hydrochloric acid-treated (HCL) pigs. The photographs have been created by digital superimposition of two color channels; PGP 9.5-positive (green) with the other studied neuronal factors (red). Neurons showing co-localization of PGP 9.5 and CART, nNOS, VIP, PACAP, SP, GAL are indicated with arrows. For abbreviations, see the description of Table 1.

Table 2. The percentage of PGP-9.5-immunoreactive prepyloric stomach enteric neurons simultaneously expressing CART, nNOS, VIP, PACAP, SP and GAL in individual control and hydrochloric acid-treated pigs

Stomach prepyloric region						
	Submucous plexus			Myenteric plexus		
		Control	HCl		Control	HCl
CART	1	4.8	23.8	1	28.6	48.2
	2	5.6	23.4	2	28.0	49.2
	3	9.0	25.6	3	42.75	54.0
	4	8.0	25.2	4	32.4	52.4
	Average	6.85 ± 0.98	24.5 ± 0.53*	Average	32.94 ± 3.41	50.95 ± 1.35*
NOS	1	3.4	19.2	1	24.2	27.6
	2	3.6	23.4	2	21.0	30.8
	3	5.2	17.0	3	15.8	26.2
	4	2.2	19.8	4	20.6	23.0
	Average	3.6 ± 0.61	19.85 ± 1.32*	Average	20.4 ± 1.73	26.9 ± 1.61
VIP	1	1.2	11.6	1	10.2	17.4
	2	3.0	9.4	2	9.4	19.0
	3	0.6	9.8	3	7.6	18.2
	4	1.6	13.8	4	6.6	16.6
	Average	1.6 ± 0.50	11.15 ± 1.00*	Average	8.45 ± 0.82	17.8 ± 0.51*
PACAP	1	0.2	13.4	1	4.2	8.4
	2	1.4	9.4	2	5.6	6.6
	3	1.8	12.2	3	1.4	8.2
	4	0.4	9.8	4	2.2	11.2
	Average	0.95 ± 0.38	11.2 ± 0.95*	Average	3.35 ± 0.95	8.6 ± 0.95
SP	1	36.2	50.4	1	8.2	12.2
	2	40.2	49.4	2	9.6	13.6
	3	41.0	55.2	3	7.2	10.8
	4	35.6	48.2	4	10.4	11.6
	Average	38.25 ± 1.37	50.8 ± 1.53*	Average	8.85 ± 0.71	9.55 ± 0.59
GAL	1	23.6	44.2	1	13.8	23.2
	2	25.8	43.4	2	10.2	19.2
	3	19.4	38.6	3	15.6	22.8
	4	22.6	40.2	4	12.4	27.4
	Average	22.85 ± 1.33	41.6 ± 1.32*	Average	13.0 ± 1.14	23.15 ± 1.67*

*For abbreviations, see the description of Table 1. Means and standard errors of the mean for each group of animals and studied antigens are provided. The significance of differences was evaluated using Student's t test for independent samples. The differences were considered statistically significant at *P ≤ 0.05.

whereas in the myenteric plexus an increase from 8% in control animals to 18% in experimental animals was noted.

PACAP was found in 1% of submucous neurons of untested animals and 11% of neurons of investigated pigs. In the myenteric plexus, PACAP-IR cells constituted 3% of the referred PGP-9.5-IR control population and 9% in HCl-treated animals.

In the submucous plexus, SP expression was found in 38% of the enteric neurons, while in experimental group it constituted 51% of the total population. The myenteric plexus contained 9% of the SP-positive cells in physiological control and 10% in the experimental group.

GAL-IR submucous nerve cells constituted 23% of the reference neurons in control animals, while

HCl treatment caused their increase to 42%. In the myenteric plexus, GAL-expressing neurons in the control group constituted 13% of the total, and in HCl-treated animals they accounted for 23%.

Gastroscopic examination of control and HCl group on the first day and control on the seventh day did not reveal any inflammatory symptoms in the gastric mucosa, while HCl group on the seventh day past gastric HCl instillation revealed inflammatory changes of the mucosa like hyperemia and superficial erosions.

Discussion

This experiment has shown, for the first time, that hyperacidity conditions cause a significant increase in the expression of CART, nNOS, VIP, PACAP, SP and GAL in the submucous gastric neurons of the pig. In the neurons of myenteric plexus, a significant increase of VIP-, CART- and GAL-immunoreactivity was found. nNOS and PACAP showed tendency to increase, although this was not statistically significant, while SP expression did not change. The current data clearly show that in the myenteric plexus SP plays a minor, if any, role in the adaptation of myenteric neurons to the hyperacidic gastric *milieu*. This finding is generally consistent with our previous report that intragastric hydrochloric acid infusion, mimicking hyperacidity state, affected the chemical plasticity of the stomach extrinsic sympathetic neurons [9]. Moreover, we identified specific neurotransmitters involved in the pathology and indicated their precise allocation in the ENS structures and chemically specific neuronal groups which participated in the adaptive response. This allocation bears functional connotation, since neurons forming myenteric plexus are thought to be responsible for control of the stomach and gut motor functions, whereas submucous neurons mainly regulate mucosal secretion [20–22]. An increased expression of the studied substances in both plexuses (except SP in the myenteric plexus) suggests that a hyperacidity-induced adaptive reaction in the stomach wall affects both secretory and motor functions.

It has been well-documented that disproportionate stress [31, 32] or gastrin upregulation [33] underlies the formation of stomach ulcers and excessive secretion of acids is conducive to the development of gastric cancer [34]. Opposing those effects, mucus and bicarbonate secretion form the first line of defense in protecting gastric epithelial cells from acids and digestive enzymes [1, 11]. It has been increasingly realized that enteric neurotransmitters are actively engaged in the regulation of both gastric acid secretion as well as the formation of the mucous barrier [35].

One of the factors suppressing gastric acid secretion is CART [12, 13]. Since its discovery in 1981, CART [36] has been reported to be present in the stomach enteric neurons of numerous species, including those particularly susceptible to ulcer formation, such as humans [27] and pigs [24]. CART has been also implicated as regulator of nitric oxide release [13]. Intriguingly, many authors have reported on the ulcer-protective influence of NO in the stomach [14, 15]. Indeed, NO is an important component of the gastroduodenal defense system due to its inhibitory effects on gastric acid secretion [37]. Moreover in the stomach, enteric neurons co-localize NOS with VIP and in isolated myenteric ganglia VIP induced NO release, and NO facilitated VIP release [38]. VIP attenuates HCl secretion *via* downregulating gastrin secretion [16]. This multi-factorial anti-acidic action is additionally supported by calcitonin-gene-related peptide (CGRP) which has been detected in the stomach neurons [26, 39]. An inhibitory action on gastric acid secretion is also exerted by GAL which was found to be overexpressed in applied here model of hyperacidity [40]. Therefore, CART-, nNOS-, VIP-, CGRP and GAL-immunoreactive enteric neurons of the submucous plexus are very likely to contribute to a complex inhibitory mechanism that prevents gastric hyperacidity and, consequently, gastric mucosal destruction. In contrast, VIP related PACAP has an opposite, stimulatory action on HCl release [16]. This opposite action of PACAP confirms the existence of a two-way neuronal inhibitory/excitatory control of the acid secretion.

Stomach epithelial functions are mainly regulated by the submucous plexus which in cooperation with primary afferent sensory neurons innervate gastric mucosal and submucosal vessels and through regulation of the mucosal blood flow affect mucosal secretion [20]. Mucus secretion protects epithelial cells from acids and digestive enzymes, abrasion by food particles, and pathogens. An increase in mucus thickness is a routine defensive response to luminal insults. Mucus traps secreted bicarbonate on the surface of the epithelium, forming a neutral pH layer that enables epithelial protection and repair [41]. Nitric oxide, a potent vasodilator [42], increases epithelial mucus secretion *via* activation of guanylyl cyclase in stomach epithelium [43]. Our study revealed increased expression of CART and SP in the submucous plexus of experimental pigs. It is clear that CART, through stimulation of NO release [13] parallelly to SP [44] may modulate local blood flow and affect mucus secretion. Indeed, the occurrence of NO-synthesizing neurons demonstrated in this study throughout the submucous plexus, coupled with its high perme-

ability range (up to 300 μm) [45], enables NO-ergic neurons to affect multiple targets in the stomach's epithelium and in the sub-epithelial layer of the mucosa which comprises blood vessels, non-epithelial cells and other enteric nerve cells.

Stomach acidification, parallel to mucus, is known to increase secretion of bicarbonate ions by the epithelium and their retention within the mucus gel layer [11]. The main role of bicarbonate is to neutralize hydrogen ions and pepsin invading from the lumen [35]. Consistently, bicarbonate secretion has been linked with CGRP-dependent NO formation and local hyperemia [46]. It was also reported that GLP-2 which is released by luminal nutrients, stimulates in human and pig tissues bicarbonate secretion *via* VIP-ergic submucous neurons which express GLP-2 receptor [47, 48]. Although this stimulation is mediated by NO-ergic pathway and comprises local hyperemia, it appears to be independent of the above-mentioned capsaicin-sensitive afferent connections [49].

In humans, vagal stimulation results in parallel bicarbonate and gastric acid secretion [50]. Available data show that PACAP stimulates bicarbonate secretion in the duodenum [38, 51] as well as gastric acid secretion in the stomach [16]. Our previous findings revealed in aspirin-evoked pig model of stomach inflammation increased expression of PACAP as well as *de novo* expression of VIP, NOS and GAL in numerous stomach-supplying perikarya located in the dorsal motor vagal nucleus (DMX) [52]. Thus, activation of the parasympathetic stomach supplying DMX-located neurons triggers interneuronal signaling mechanisms which promote the release of the neurotransmitters into the gastric submucosal space. In the light of these findings, vagal mediators PACAP, VIP, NO and GAL released into submucosal space are likely to affect multiple aspects of the gastric secretion and possibly the function of enteric neurons. The fact that PACAP, VIP, NO and GAL are up-regulated simultaneously in vagal DMX, as well as myenteric and submucous neurons indicates their complementary role in the adaptive neuronal processes, including hyperacidity-evoked gastritis. Nevertheless, the exact role of particular mediators still remains unclear and deserves further exploration.

Gastric motility is regulated by neural circuits that affect smooth muscle contractility. Current studies have shown that the gastric inhibitory vagal motor circuit that comprises DMX-located preganglionic cholinergic neurons and postganglionic neurons of the myenteric plexus also mediates inhibition of gastric emptying [53]. Vagal stimulation of the myenteric neurons relaxes the smooth muscles by releasing VIP and NO [54]. This increased relaxation may account

for gastrointestinal motility disorders [38]. Thus, as revealed in the current experiment, the hyperacidity-evoked increased expression of VIP and NOS in myenteric neurons is congruent with the above hypothesis, especially in view of delayed gastric emptying accompanying hyperacidity-induced gastric and duodenal ulcers [29].

In conclusion, this study disclosed that stomach hyperacidity in a specific way modifies the expression of CART, nNOS, VIP, PACAP, SP and GAL in the porcine gastric neurons. Increased expression of the majority of the studied biologically active substances in both the submucous and myenteric plexuses points to the complexity of neural regulation of the gastric response to hyperacidity. The current data strongly support functional studies indicating an active role of the studied neuromodulators in local blood flow regulation, control of gastric acid secretion, mucous/bicarbonate layer formation, control of stomach motility, inflammation and neuroprotection. Nevertheless, further studies are needed to reveal exact mechanisms of regulatory action of the studied neurotransmitters in the stomach prepyloric region.

Funding

Grant of the Polish State Committee for Scientific Research number 1890/B/P01/2010/39; the University of Warmia and Mazury in Olsztyn (statutory research) grant No.15.610.003-300; KNOW (Leading National Research Centre) Scientific Consortium "Healthy Animal — Safe Food", decision of Ministry of Science and Higher Education No. 05-1/KNOW2/2015; Project financially co-supported by Minister of Science and Higher Education in the range of the program entitled "Regional Initiative of Excellence" for the years 2019–2020, Project No. 010/RID/2018/19.

Acknowledgments

The author appreciates the excellent technical assistance of veterinarian Liliana Rytel and Andrzej Pobjedzinski, M.Sc.

References

1. Højgaard L, Mertz Nielsen A, Rune SJ. Peptic ulcer pathophysiology: acid, bicarbonate, and mucosal function. *Scand J Gastroenterol Suppl.* 1996; 216: 10–15, doi: [10.3109/00365529609094555](https://doi.org/10.3109/00365529609094555), indexed in Pubmed: 8726273.
2. Schubert ML. Functional anatomy and physiology of gastric secretion. *Curr Opin Gastroenterol.* 2015; 31(6): 479–485, doi: [10.1097/MOG.0000000000000213](https://doi.org/10.1097/MOG.0000000000000213), indexed in Pubmed: 26376477.
3. Alventosa-Mateu C, Ferrer-Barceló L, Huguet-Malavés JM, et al. Zollinger-Ellison syndrome. *Rev Esp Enferm Dig.* 2013; 105(10): 641–642, doi: [10.4321/s1130-01082013001000016](https://doi.org/10.4321/s1130-01082013001000016), indexed in Pubmed: 24641468.

4. Dacha S, Razvi M, Massaad J, et al. Hypergastrinemia. *Gastroenterol Rep (Oxf)*. 2015; 3(3): 201–208, doi: [10.1093/gastro/gov004](https://doi.org/10.1093/gastro/gov004), indexed in Pubmed: [25698559](https://pubmed.ncbi.nlm.nih.gov/25698559/).
5. Phan J, Benhammou JN, Pisegna JR. Gastric hypersecretory states: investigation and management. *Curr Treat Options Gastroenterol*. 2015; 13(4): 386–397, doi: [10.1007/s11938-015-0065-8](https://doi.org/10.1007/s11938-015-0065-8), indexed in Pubmed: [26342486](https://pubmed.ncbi.nlm.nih.gov/26342486/).
6. Arafa Keshk W, Zahran SM, Katary MA, et al. Modulatory effect of silymarin on nuclear factor-erythroid-2-related factor 2 regulated redox status, nuclear factor- κ B mediated inflammation and apoptosis in experimental gastric ulcer. *Chem Biol Interact*. 2017; 273: 266–272, doi: [10.1016/j.cbi.2017.06.022](https://doi.org/10.1016/j.cbi.2017.06.022), indexed in Pubmed: [28648817](https://pubmed.ncbi.nlm.nih.gov/28648817/).
7. Magierowski M, Magierowska K, Hubalewska-Mazgaj M, et al. Cross-talk between hydrogen sulfide and carbon monoxide in the mechanism of experimental gastric ulcers healing, regulation of gastric blood flow and accompanying inflammation. *Biochem Pharmacol*. 2018; 149: 131–142, doi: [10.1016/j.bcp.2017.11.020](https://doi.org/10.1016/j.bcp.2017.11.020), indexed in Pubmed: [29203367](https://pubmed.ncbi.nlm.nih.gov/29203367/).
8. Taylor S, Spugnini EP, Assaraf YG, et al. Microenvironment acidity as a major determinant of tumor chemoresistance: Proton pump inhibitors (PPIs) as a novel therapeutic approach. *Drug Resist Updat*. 2015; 23: 69–78, doi: [10.1016/j.drug.2015.08.004](https://doi.org/10.1016/j.drug.2015.08.004), indexed in Pubmed: [26341193](https://pubmed.ncbi.nlm.nih.gov/26341193/).
9. Palus K, Calka J. Neurochemical plasticity of the coeliac-superior mesenteric ganglion complex neurons projecting to the prepyloric area of the porcine stomach following hyperacidity. *Neural Plast*. 2016; 2016: 8596214, doi: [10.1155/2016/8596214](https://doi.org/10.1155/2016/8596214), indexed in Pubmed: [27293908](https://pubmed.ncbi.nlm.nih.gov/27293908/).
10. Holzer P. Neural emergency system in the stomach. *Gastroenterology*. 1998; 114(4): 823–839, doi: [10.1016/s0016-5085\(98\)70597-9](https://doi.org/10.1016/s0016-5085(98)70597-9).
11. Yandrapu H, Sarosiek J. Protective factors of the gastric and duodenal mucosa: an overview. *Curr Gastroenterol Rep*. 2015; 17(6): 24, doi: [10.1007/s11894-015-0452-2](https://doi.org/10.1007/s11894-015-0452-2), indexed in Pubmed: [26109006](https://pubmed.ncbi.nlm.nih.gov/26109006/).
12. Okumura T, Yamada H, Motomura W, et al. Cocaine-amphetamine-regulated transcript (CART) acts in the central nervous system to inhibit gastric acid secretion via brain corticotropin-releasing factor system. *Endocrinology*. 2000; 141(8): 2854–2860, doi: [10.1210/endo.141.8.7588](https://doi.org/10.1210/endo.141.8.7588), indexed in Pubmed: [10919272](https://pubmed.ncbi.nlm.nih.gov/10919272/).
13. Ekblad E. CART in the enteric nervous system. *Peptides*. 2006; 27(8): 2024–2030, doi: [10.1016/j.peptides.2005.12.015](https://doi.org/10.1016/j.peptides.2005.12.015), indexed in Pubmed: [16759747](https://pubmed.ncbi.nlm.nih.gov/16759747/).
14. Czekaj R, Majka J, Ptak-Belowska A, et al. Role of curcumin in protection of gastric mucosa against stress-induced gastric mucosal damage. Involvement of hypoacidity vasoactive mediators and sensory neuropeptides. *J Physiol Pharmacol*. 2016; 67:261–275, indexed in Pubmed: [27226186](https://pubmed.ncbi.nlm.nih.gov/27226186/).
15. Sepulveda B, Quispe C, Simirgiotis M, et al. Gastroprotective activity of synthetic coumarins: Role of endogenous prostaglandins, nitric oxide, non-protein sulfhydryls and vanilloid receptors. *Bioorg Med Chem Lett*. 2016; 26(23): 5732–5735, doi: [10.1016/j.bmcl.2016.10.056](https://doi.org/10.1016/j.bmcl.2016.10.056), indexed in Pubmed: [27810240](https://pubmed.ncbi.nlm.nih.gov/27810240/).
16. Zeng N, Athmann C, Kang T, et al. PACAP type I receptor activation regulates ECL cells and gastric acid secretion. *J Clin Invest*. 1999; 104(10): 1383–1391, doi: [10.1172/JCI7537](https://doi.org/10.1172/JCI7537), indexed in Pubmed: [10562300](https://pubmed.ncbi.nlm.nih.gov/10562300/).
17. Laine L, Takeuchi K, Tarnawski A. Gastric mucosal defense and cytoprotection: bench to bedside. *Gastroenterology*. 2008; 135(1): 41–60, doi: [10.1053/j.gastro.2008.05.030](https://doi.org/10.1053/j.gastro.2008.05.030), indexed in Pubmed: [18549814](https://pubmed.ncbi.nlm.nih.gov/18549814/).
18. Matteo F, Luca A, Rocchina C, et al. Matteo F, Luca A, Rocchina C, Marco T, Corrado B. Pathophysiology of gastric ulcer development and healing: Molecular mechanisms and novel therapeutic options. In: Chai J Ed. *Peptic ulcer disease*. 2011; 113–142.
19. Makowska K, Gonkowski S, Zielonka L, et al. T2 toxin-induced changes in cocaine- and amphetamine-regulated transcript (CART)-like immunoreactivity in the enteric nervous system within selected fragments of the porcine digestive tract. *Neurotox Res*. 2017; 31(1): 136–147, doi: [10.1007/s12640-016-9675-8](https://doi.org/10.1007/s12640-016-9675-8), indexed in Pubmed: [27738989](https://pubmed.ncbi.nlm.nih.gov/27738989/).
20. Krueger D, Michel K, Zeller F, et al. Neural influences on human intestinal epithelium in vitro. *J Physiol*. 2016; 594(2): 357–372, doi: [10.1113/JP271493](https://doi.org/10.1113/JP271493), indexed in Pubmed: [26527433](https://pubmed.ncbi.nlm.nih.gov/26527433/).
21. Burnstock G. The innervation of the gut of the brown trout *salmo trutta*. *Q J Microsc Sci*. 1959; 100: 199–220.
22. Olsson C. Autonomic innervation of the fish gut. *Acta Histochem*. 2009; 111(3): 185–195, doi: [10.1016/j.acthis.2008.11.014](https://doi.org/10.1016/j.acthis.2008.11.014), indexed in Pubmed: [19124149](https://pubmed.ncbi.nlm.nih.gov/19124149/).
23. Vasina V, Barbara G, Talamonti L, et al. Enteric neuroplasticity evoked by inflammation. *Auton Neurosci*. 2006; 126-127: 264–272, doi: [10.1016/j.autneu.2006.02.025](https://doi.org/10.1016/j.autneu.2006.02.025), indexed in Pubmed: [16624634](https://pubmed.ncbi.nlm.nih.gov/16624634/).
24. Bulc M, Gonkowski S, Calka J. Expression of cocaine and amphetamine regulated transcript (cart) in the porcine intramural neurons of stomach in the course of experimentally induced diabetes mellitus. *J Mol Neurosci*. 2015; 57(3): 376–385, doi: [10.1007/s12031-015-0618-2](https://doi.org/10.1007/s12031-015-0618-2), indexed in Pubmed: [26266486](https://pubmed.ncbi.nlm.nih.gov/26266486/).
25. Burliański PJ, Rychlik A, Calka J. Effects of inflammation and axotomy on expression of acetylcholine transferase and nitric oxide synthetase within the cocaine- and amphetamine-regulated transcript-immunoreactive neurons of the porcine descending colon. *J Comp Pathol*. 2014; 150(2-3): 287–296, doi: [10.1016/j.jcpa.2013.08.007](https://doi.org/10.1016/j.jcpa.2013.08.007), indexed in Pubmed: [24650891](https://pubmed.ncbi.nlm.nih.gov/24650891/).
26. Kaleczyc J, Klimczuk M, Franke-Radowiecka A, et al. The distribution and chemical coding of intramural neurons supplying the porcine stomach - the study on normal pigs and on animals suffering from swine dysentery. *Anat Histol Embryol*. 2007; 36(3): 186–193, doi: [10.1111/j.1439-0264.2006.00744.x](https://doi.org/10.1111/j.1439-0264.2006.00744.x), indexed in Pubmed: [17535350](https://pubmed.ncbi.nlm.nih.gov/17535350/).
27. Kasacka I, Piotrowska Z, Car H, et al. Cocaine- and amphetamine-regulated transcript: identification and distribution in human gastrointestinal tract. *J Biol Regul Homeost Agents*. 2012; 26(3): 419–428, indexed in Pubmed: [23034261](https://pubmed.ncbi.nlm.nih.gov/23034261/).
28. Iijima K, Kanno T, Abe Y, et al. Preferential location of idiopathic peptic ulcers. *Scand J Gastroenterol*. 2016; 51(7): 782–787, doi: [10.3109/00365521.2016.1141316](https://doi.org/10.3109/00365521.2016.1141316), indexed in Pubmed: [26854021](https://pubmed.ncbi.nlm.nih.gov/26854021/).
29. Kanaizumi T, Nakano H, Matsui T, et al. Gastric emptying in patients with gastric and duodenal ulcer. *Tohoku J Exp Med*. 1989; 158(2): 133–140, doi: [10.1620/tjem.158.133](https://doi.org/10.1620/tjem.158.133), indexed in Pubmed: [2772918](https://pubmed.ncbi.nlm.nih.gov/2772918/).
30. Verma N, Rettenmeier AW, Schmitz-Spanke S. Recent advances in the use of *Sus scrofa* (pig) as a model system for proteomic studies. *Proteomics*. 2011; 11(4): 776–793, doi: [10.1002/pmic.201000320](https://doi.org/10.1002/pmic.201000320), indexed in Pubmed: [21229584](https://pubmed.ncbi.nlm.nih.gov/21229584/).
31. File SE, Pearce JB. Benzodiazepines reduce gastric ulcers induced in rats by stress. *Br J Pharmacol*. 1981; 74(3): 593–599, doi: [10.1111/j.1476-5381.1981.tb10469.x](https://doi.org/10.1111/j.1476-5381.1981.tb10469.x), indexed in Pubmed: [7296164](https://pubmed.ncbi.nlm.nih.gov/7296164/).
32. Paré W, Glavin G. Restraint stress in biomedical research: A review. *Neurosci Biobehav Rev*. 1986; 10(3): 339–370, doi: [10.1016/0149-7634\(86\)90017-5](https://doi.org/10.1016/0149-7634(86)90017-5), indexed in Pubmed: [3095718](https://pubmed.ncbi.nlm.nih.gov/3095718/).
33. Sun FP, Song YG, Cheng W, et al. Gastrin, somatostatin, G and D cells of gastric ulcer in rats. *World J Gastroenterol*. 2002; 8(2): 375–378, doi: [10.3748/wjg.v8.i2.375](https://doi.org/10.3748/wjg.v8.i2.375), indexed in Pubmed: [11925629](https://pubmed.ncbi.nlm.nih.gov/11925629/).

34. Zhou S, Yao D, Guo L, et al. Curcumin suppresses gastric cancer by inhibiting gastrin-mediated acid secretion. *FEBS Open Bio*. 2017; 7(8): 1078–1084, doi: [10.1002/2211-5463.12237](https://doi.org/10.1002/2211-5463.12237), indexed in Pubmed: [28781948](https://pubmed.ncbi.nlm.nih.gov/28781948/).
35. Allen A, Flemström G. Gastroduodenal mucus bicarbonate barrier: protection against acid and pepsin. *Am J Physiol Cell Physiol*. 2005; 288(1): C1–19, doi: [10.1152/ajpcell.00102.2004](https://doi.org/10.1152/ajpcell.00102.2004), indexed in Pubmed: [15591243](https://pubmed.ncbi.nlm.nih.gov/15591243/).
36. Spiess J, Villarreal J, Vale W. Isolation and sequence analysis of a somatostatin-like polypeptide from ovine hypothalamus. *Biochemistry*. 2002; 20(7): 1982–1988, doi: [10.1021/bi00510a038](https://doi.org/10.1021/bi00510a038).
37. Kemmerly T, Kaunitz JD. Gastroduodenal mucosal defense. *Curr Opin Gastroenterol*. 2014; 30(6): 583–588, doi: [10.1097/MOG.000000000000124](https://doi.org/10.1097/MOG.000000000000124), indexed in Pubmed: [25229259](https://pubmed.ncbi.nlm.nih.gov/25229259/).
38. Van Geldre LA, Lefebvre RA. Interaction of NO and VIP in gastrointestinal smooth muscle relaxation. *Curr Pharm Des*. 2004; 10(20): 2483–2497, doi: [10.2174/1381612043383890](https://doi.org/10.2174/1381612043383890), indexed in Pubmed: [15320758](https://pubmed.ncbi.nlm.nih.gov/15320758/).
39. Helton WS, Mulholland MM, Bunnett NW, et al. Inhibition of gastric and pancreatic secretion in dogs by CGRP: role of somatostatin. *Am J Physiol*. 1989; 256(4 Pt 1): G715–G720, doi: [10.1152/ajpgi.1989.256.4.G715](https://doi.org/10.1152/ajpgi.1989.256.4.G715), indexed in Pubmed: [2565089](https://pubmed.ncbi.nlm.nih.gov/2565089/).
40. Norlén P, Bernsand M, Konagaya T, et al. ECL-cell histamine mobilization in conscious rats: effects of locally applied regulatory peptides, candidate neurotransmitters and inflammatory mediators. *Br J Pharmacol*. 2001; 134(8): 1767–1777, doi: [10.1038/sj.bjp.0704419](https://doi.org/10.1038/sj.bjp.0704419), indexed in Pubmed: [11739254](https://pubmed.ncbi.nlm.nih.gov/11739254/).
41. Wallace JL, Ianaro A, de Nucci G. Gaseous mediators in gastrointestinal mucosal defense and injury. *Dig Dis Sci*. 2017; 62(9): 2223–2230, doi: [10.1007/s10620-017-4681-0](https://doi.org/10.1007/s10620-017-4681-0), indexed in Pubmed: [28733867](https://pubmed.ncbi.nlm.nih.gov/28733867/).
42. Moncada S. Nitric oxide. *J Hypertens Suppl*. 1994; 12: S35–39, indexed in Pubmed: [7539493](https://pubmed.ncbi.nlm.nih.gov/7539493/).
43. Brown J, Hanson P, Whittle B. Nitric oxide donors increase mucus gel thickness in rat stomach. *Eur J Pharmacol*. 1992; 223(1): 103–104, doi: [10.1016/0014-2999\(92\)90824-n](https://doi.org/10.1016/0014-2999(92)90824-n), indexed in Pubmed: [1335874](https://pubmed.ncbi.nlm.nih.gov/1335874/).
44. Walsh DA, McWilliams D. Tachykinins and the cardiovascular system. *Curr Drug Targets*. 2006; 7(8): 1031–1042, doi: [10.2174/138945006778019291](https://doi.org/10.2174/138945006778019291), indexed in Pubmed: [16918331](https://pubmed.ncbi.nlm.nih.gov/16918331/).
45. Garthwaite J, Boulton CL. Nitric Oxide Signaling in the Central Nervous System. *Ann Rev Physiol*. 1995; 57(1): 683–706, doi: [10.1146/annurev.ph.57.030195.003343](https://doi.org/10.1146/annurev.ph.57.030195.003343).
46. Abdel-Salam OM, Debrececi A, Mózsik G, et al. Capsaicin-sensitive afferent sensory nerves in modulating gastric mucosal defense against noxious agents. *J Physiol Paris*. 1999; 93(5): 443–454, doi: [10.1016/s0928-4257\(99\)00115-1](https://doi.org/10.1016/s0928-4257(99)00115-1), indexed in Pubmed: [10674923](https://pubmed.ncbi.nlm.nih.gov/10674923/).
47. Guan X, Karpen HE, Stephens J, et al. GLP-2 receptor localizes to enteric neurons and endocrine cells expressing vasoactive peptides and mediates increased blood flow. *Gastroenterology*. 2006; 130(1): 150–164, doi: [10.1053/j.gastro.2005.11.005](https://doi.org/10.1053/j.gastro.2005.11.005), indexed in Pubmed: [16401478](https://pubmed.ncbi.nlm.nih.gov/16401478/).
48. Kaji I, Akiba Y, Kaunitz JD. Digestive physiology of the pig symposium: involvement of gut chemosensing in the regulation of mucosal barrier function and defense mechanisms. *J Anim Sci*. 2013; 91(5): 1957–1962, doi: [10.2527/jas.2012-5941](https://doi.org/10.2527/jas.2012-5941), indexed in Pubmed: [23345558](https://pubmed.ncbi.nlm.nih.gov/23345558/).
49. Wang JH, Inoue T, Higashiyama M, et al. Umami receptor activation increases duodenal bicarbonate secretion via glucagon-like peptide-2 release in rats. *J Pharmacol Exp Ther*. 2011; 339(2): 464–473, doi: [10.1124/jpet.111.184788](https://doi.org/10.1124/jpet.111.184788), indexed in Pubmed: [21846840](https://pubmed.ncbi.nlm.nih.gov/21846840/).
50. Forssell H, Stenquist B, Olbe L. Vagal stimulation of human gastric bicarbonate secretion. *Gastroenterology*. 1985; 89(3): 581–586, doi: [10.1016/0016-5085\(85\)90454-8](https://doi.org/10.1016/0016-5085(85)90454-8), indexed in Pubmed: [3926592](https://pubmed.ncbi.nlm.nih.gov/3926592/).
51. Takeuchi K, Yagi K, Sugamoto S, et al. Involvement of PACAP in acid-induced HCO₃⁻ response in rat duodenum. *Pharmacol Res*. 1998; 38(6): 475–480, doi: [10.1006/phrs.1998.0393](https://doi.org/10.1006/phrs.1998.0393), indexed in Pubmed: [9990657](https://pubmed.ncbi.nlm.nih.gov/9990657/).
52. Gaňko M, Čařka J. Prolonged acetylsalicylic-acid-supplementation-induced gastritis affects the chemical coding of the stomach innervating vagal efferent neurons in the porcine dorsal motor vagal nucleus (DMX). *J Mol Neurosci*. 2014; 54(2): 188–198, doi: [10.1007/s12031-014-0274-y](https://doi.org/10.1007/s12031-014-0274-y), indexed in Pubmed: [24643520](https://pubmed.ncbi.nlm.nih.gov/24643520/).
53. Goyal RK, Guo Y, Mashimo H. Advances in the physiology of gastric emptying. *Neurogastroenterol Motil*. 2019; 31(4): e13546, doi: [10.1111/nmo.13546](https://doi.org/10.1111/nmo.13546), indexed in Pubmed: [30740834](https://pubmed.ncbi.nlm.nih.gov/30740834/).
54. He XD, Goyal RK. Nitric oxide involvement in the peptide VIP-associated inhibitory junction potential in the guinea-pig ileum. *J Physiol*. 1993; 461(1): 485–499, doi: [10.1113/jphysiol.1993.sp019524](https://doi.org/10.1113/jphysiol.1993.sp019524), indexed in Pubmed: [8102401](https://pubmed.ncbi.nlm.nih.gov/8102401/).

Submitted: 4 December, 2019

Accepted after reviews: 11 December, 2019

Available as AoP: 16 December, 2019

**The Editors are highly indebted to the following Reviewers
of the volume 57 (2019) of FHC**

Folia Histochemica et Cytobiologica

Scientific quarterly devoted to problems of histochemistry,
cytochemistry and cell & tissue biology

www.fhc.viamedica.pl

Vol. 57

No. 1–4

2019

Official Journal of the Polish Society for Histochemistry and Cytochemistry

CONTENTS

No. 1

REVIEW

***In vitro* generation of pancreatic β -cells for diabetes treatment. I. β -like cells derived from human pluripotent stem cells**

Katarzyna Cierpka-Kmieć, Agata Wronska, Zbigniew Kmieć 1

ORIGINAL PAPERS

The impact of sedentary work on sperm nuclear DNA integrity

Kamil Gill, Joanna Jakubik, Michał Kups, Aleksandra Rosiak-Gill, Rafał Kurzawa,
Maciej Kurpisz, Monika Fraczek, Małgorzata Piasecka 15

Immunohistochemical demonstration of LH/CG receptors in non-neoplastic human adrenal cortex and adrenocortical tumors

Piotr Korol, Maria Jaranowska, Marek Pawlikowski 23

The role of CD44H molecule in the interactions between human monocytes and pancreatic adenocarcinoma-derived microvesicles

Monika Baj-Krzyworzeka, Kazimierz Weglarczyk, Rafał Szatanek, Bożenna Mytar, Jarosław Baran, Maciej Siedlar 28

CASE REPORT

The role of immunohistochemical examination in diagnosis of papillary thyroid cancer in struma ovarii

Ewelina Szczepanek-Parulska, Anna Pioch, Ewa Cyranska-Chyrek, Kosma Wolinski,
Donata Jarmolowska-Jurczyszyn, Małgorzata Janicka-Jedynska, Przemysław Majewski,
Maciej Zabel, Marek Ruchala 35

No. 2

REVIEW PAPER

MPP1-based mechanism of resting state raft organization in the plasma membrane. Is it a general or specialized mechanism in erythroid cells?

Magdalena Trybus, Lukasz Niemiec, Agnieszka Biernatowska,
Anita Hryniewicz-Jankowska, Aleksander F. Sikorski 43

ORIGINAL PAPERS

L1-ORF1p and Ago2 are involved in a siRNA-mediated regulation for promoter activity of L1-5'UTR

Liu Shi, Huanhuan Shi, Liangliang Lou, Xiaoning Yuan, Yunfeng Zhu 56

The miR-1204 regulates apoptosis in NSCLC cells by targeting DEK

Zhen Qian, Juan Yang, Huanhuan Liu, Yue Yin, Lingling Hou, Honggang Hu 64

The immunoreactivity of TGF- β 1 in non-alcoholic fatty liver disease

Radoslaw Kempinski, Katarzyna Neubauer, Elzbieta Poniewierka, Maciej Kaczorowski, Agnieszka Halon 74

WNT5A gene and protein expression in endometrial cancer

Tomasz Wasniewski, Jacek Kiezun, Bartłomiej E. Krazinski Anna E. Kowalczyk,
Blazej Szostak, Piotr M. Wierzbicki, Jolanta Kiewisz 84

Gallbladder interstitial Cajal-like cells and gallbladder contractility in patients with cholelithiasis: a prospective study

Runyu Ding, Junmin Wei, Jingyong Xu 94

No. 3

REVIEW PAPER

Pancreatic β -cell replacement: advances in protocols used for differentiation of pancreatic progenitors to β -like cells

Muhammad Waseem Ghani, Li Ye, Zhao Yi, Hammad Ghani, Muhammad Waseem Birmani,
Aamir Nawab, Lang Guan Cun, Liu Bin, Xiao Mei 101

ORIGINAL PAPERS

Cytoplasmic and membranous receptor-binding cancer antigens expressed on SiSo cells (RCAS1) immunoreactivity in epithelial ovarian cancer cells represent differing biological function of RCAS1

Sebastian Szubert, Wojciech Jozwicki, Lukasz Wicherek, Krzysztof Koper 116

Stem cells and metformin synergistically promote healing in experimentally induced cutaneous wound injury in diabetic rats

Lamiaa M. Shawky, Eman A. El Bana, Ahmed A. Morsi 127

Nucleolin and nucleophosmin expression in seminomas and non-seminomatous testicular tumors

Marek Masiuk, Magdalena Lewandowska, Leszek Teresinski, Ewa Dobak, Elzbieta Urasinska 139

Diagnostic immunohistochemistry for canine cutaneous round cell tumours — retrospective analysis of 60 cases

Katarzyna Pazdzior-Czapula, Mateusz Mikiewicz, Michal Gesek, Cezary Zwolinski, Iwona Otrocka-Domagala 146

No. 4

OBITUARY

Professor Stanisława Stokłosowa (1927–2019)

Barbara Bilinska, Jerzy Galas, Andrzej Lukaszzyk, Jerzy Kawiak 155

COMMENTARY

Transforming growth factor- β activation in cell-free extracellular matrix preparations. Commentary

John R. Couchman..... 157

ORIGINAL PAPERS

In vitro evaluation of electroporated gold nanoparticles and extremely-low frequency electromagnetic field anticancer activity against Hep-2 laryngeal cancer cells

Mohammed A. Alshehri, Piotr M. Wierzbicki, Hassan F. Kaboo, Mohamed S.M. Nasr, Mohamed E. Amer, Tamer M.M. Abuamara, Doaa A. Badr, Kamel A. Saleh, Ahmed E. Fazary, Aly F. Mohamed..... 159

MiR-539-5p alleviates sepsis-induced acute lung injury by targeting ROCK1

Li Meng, Haohao Cao, Chunhua Wan, Lintao Jiang..... 168

Increased expression of CART, nNOS, VIP, PACAP, SP and GAL in enteric neurons of the porcine stomach prepyloric region following hydrochloric acid infusion

Jaroslav Calka..... 179

INSTRUCTIONS FOR AUTHORS

MANUSCRIPT SUBMISSION

Folia Histochemica et Cytobiologica accepts manuscripts (original articles, short communications, review articles) from the field of histochemistry, as well as cell and tissue biology. Each manuscript is reviewed by independent referees. Book reviews and information concerning congresses, symposia, meetings etc., are also published.

All articles should be submitted to FHC electronically online at www.fhc.viamedica.pl where detailed instruction regarding submission process will be provided.

AUTHOR'S STATEMENT

The manuscript must be accompanied by the author's statement that it has not been published (or submitted to publication) elsewhere.

GHOSTWRITING

Ghostwriting and guest-authorship are forbidden. In case of detecting ghost written manuscripts, their actions will be taking involving both the submitting authors and the participants involved.

The corresponding author must have obtained permission from all authors for the submission of each version of the paper and for any change in authorship. Submission of a paper that has not been approved by all authors may result in immediate rejection.

COST OF PUBLICATION

The cost of publication of accepted manuscript is 800 Euro.

OFFPRINTS

PDF file of each printed paper is supplied for the author free of charge. Orders for additional offprints should be sent to the Editorial Office together with galley proofs.

ORGANIZATION OF MANUSCRIPT

The first page must include: the title, name(s) of author(s), affiliation(s), short running head (no more than 60 characters incl. spaces) and detailed address for correspondence including e-mail. Organization of the manuscript: 1. Abstract (not exceeding one typed page — should consist of the following sections: Introduction, Material and methods, Results, Conclusions); 2. Key words (max. 10); Introduction; Material and methods; Results; Discussion; Acknowledgements (if any); References; Tables (with legends); Figures; Legends to figures.

In a short communication, Results and Discussion should be written jointly. Organization of a review article is free.

TECHNICAL REQUIREMENTS

Illustrations (line drawings and halftones) — either single or mounted in the form of plates, can be 85 mm, 125 mm, or 175 mm wide and cannot exceed the size of 175 × 250 mm. The authors are requested to plan their illustrations in such a way that the printed area is economically used. Numbers, inscriptions and abbreviations on the figures must be about 3 mm high. In case of micrographs, magnification (e.g. × 65 000) should be given in the legend. Calibration bars can also be used. For the best quality of illustrations please provide images in one of commonly used formats e.g. *.tiff,

*.png, *.pdf (preferred resolution 300 dpi). Color illustrations can be published only at author's cost and the cost estimate will be sent to the author after submission of the manuscript. Tables should be numbered consecutively in Arabic numerals and each table must be typed on a separate page. The authors are requested to mark the places in the text, where a given table or figure should appear in print. Legends must begin on a new page and should be as concise as necessary for a self-sufficient explanation of the illustrations. PDF file of each paper is supplied free of charge.

CITATIONS

In References section of article please use following American Medical Association 9th Ed. citation style. Note, that items are listed numerically in the order they are cited in the text, not alphabetically. If you are using a typewriter and cannot use italics, then use underlining.

Authors: use initials of first and second names with no spaces. Include up to six authors. If there are more than six, include the first three, followed by et al. If no author is given, start with the title. **Books:** include the edition statement (ex: 3rd ed. or Rev ed.) between the title and place if it is not the first edition. **Place:** use abbreviations of states, not postal codes. **Journals:** abbreviate titles as shown in *Index Medicus*. If the journal does not paginate continuously through the volume, include the month (and day). **Websites:** include the name of the webpage, the name of the entire website, the full date of the page (if available), and the date you looked at it. The rules concerning a title within a title are *not* displayed here for purposes of clarity. See the printed version of the manual for details. For documents and situations not listed here, see the printed version of the manual.

EXAMPLES

Book:

1. Okuda M, Okuda D. *Star Trek Chronology: The History of the Future*. New York: Pocket Books; 1993.

Journal or Magazine Article (with volume numbers):

2. Redon J, Cifkova R, Laurent S et al. Mechanisms of hypertension in the cardiometabolic syndrome. *J Hypertens*. 2009; 27(3):441–451. doi: 10.1097/HJH.0b013e32831e13e5.

Book Article or Chapter:

3. James NE. Two sides of paradise: the Eden myth according to Kirk and Spock. In: Palumbo D, ed. *Spectrum of the Fantastic*. Westport, Conn: Greenwood; 1988:219–223.

When the manufacturers of the reagents etc. are mentioned for the first time, town, (state in the US) and country must be provided whereas for next referral only the name of the firm should be given.

Website:

4. Lynch T. DSN trials and tribble-ations review. Psi Phi: Bradley's Science Fiction Club Web site. 1996. Available at: <http://www.bradley.edu/campusorg/psiphi/DS9/ep/503r.htm>. Accessed October 8, 1997.

Journal Article on the Internet:

5. McCoy LH. Respiratory changes in Vulcans during pon farr. *J Extr Med* [serial online]. 1999;47:237–247. Available at: http://infotrac.galegroup.com/itweb/nysl_li_liu. Accessed April 7, 1999.

